Conflict of interest: none declared.

Funding

This study was supported in part by funds from the Department of Veterans Affairs (J.L.M.), and the Ministry of Education, Culture, Sports, Science and Technology of Japan; the Ministry of Health, Labour and Welfare of Japan; and the National Institute of Biomedical Innovation, Japan (T.S.).

References

1. Steinberg D. Lipoproteins and the pathogenesis of atherosclerosis. *Circulation* 1987;**76**:508–514.
2. Ross R, Glomset JA. Atherosclerosis and the arterial smooth muscle cell. Proliferation of smooth muscle is a key event in the genesis of the lesions of atherosclerosis. *Science* 1973;**180**:1332–1339.
3. Libby P. Inflammatory and immunomechanism in atherogenesis. *Atheroscler Rev* 1990;**21**:79–89.
4. Schulze PC, Lee RT. Oxidative stress and atherosclerosis. *Curr Atheroscler Rep* 2005;**7**:242–248.
5. Kunz J. Matrix metalloproteinases and atherogenesis in dependence of age. *Gerontology* 2007;**53**:63–73.
6. Mehta JL, Chen J, Hermonat PL, Romeo F, Novelli G. Lectin-like oxidized-low density lipoprotein receptor-1 (LOX-1): a critical player in the development of atherosclerosis and related disorders. *Cardiovasc Res* 2006;**69**:36–45.
7. Chen K, Chen J, Liu Y, Xie J, Li D, Sawamura T *et al.* Adhesion molecule expression in fibroblasts: alteration in fibroblast biology after transfection with LOX-1 plasmids. *Hypertension* 2005;**46**:622–627.
8. Hu CP, Dandapat A, Liu Y, Hermonat PL, Mehta JL. Blockade of hypoxia-reoxygenation-mediated collagen type I expression and MMP activity by over-expression of TGFβ1 in mouse cardiomyocytes. *Am J Physiol Heart Circ Physiol* 2007;**293**:H1833–H1838.
9. Hu CP, Dandapat A, Chen J, Fujita Y, Inoue N, Kawase Y *et al.* LOX-1 deletion alters signals of myocardial remodeling immediately after ischemia-reperfusion. *Cardiovasc Res* 2007;**76**:292–302.
10. Mehta JL, Sanada N, Hu CP, Chen J, Dandapat A, Sugawara F *et al.* Deletion of LOX-1 reduces atherogenesis in LDLR knockout mice fed high cholesterol diet. *Circ Res* 2007;**100**:1634–1642.
11. Kossmehl P, Schonberger J, Shakibaei M, Faramarzi S, Kurth E, Habighorst B *et al.* Increase of fibronectin and osteopontin in porcine hearts following ischemia and reperfusion. *J Mol Med* 2005;**83**:626–637.
12. Heeneman S, Cleutjens JP, Faber BC, Creemers EE, van Suylen R-J, Lutgens E *et al.* The dynamic extracellular matrix: intervention strategies during heart failure and atherosclerosis. *J Pathol* 2003;**200**: 516–525.
13. Schulze PC, Lee RT. Oxidative stress and atherosclerosis. *Curr Atheroscler Rep* 2005;**7**:242–248.
14. Reiss AB, Glass AD. Atherosclerosis: immune and inflammatory aspects. *J Investig Med* 2006;**54**:123–131.
15. Morita T. Heme-oxygenase and atherosclerosis. *Arterioscler Thromb Vasc Biol* 2005;**25**:1786–1795.
16. Wu BJ, Kathir K, Witting PK, Beck K, Choy K, Li C *et al.* Antioxidants protect from atherosclerosis by a heme oxygenase-1 pathway that is independent of free radical scavenging. *J Exp Med* 2006;**203**:1117–1127.
17. Shin J, Edelberg JE, Hong MK. Vulnerable atherosclerotic plaque: clinical implications. *Curr Vasc Pharmacol* 2003;**1**:183–204.
18. Herbert CS, Chandler AB, Dinsmore RE, Fuster V, Glagov S, Insull W *et al.* A definition of advanced types of atherosclerotic lesions and a histological classification of atherosclerosis. *Circulation* 1995;**92**:1355–1374.
19. Nadkarni SK, Pierce MC, Park BH, de Boer JF, Whittaker P, Bouma BE *et al.* Measurement of collagen and smooth muscle cell content in atherosclerotic plaques using polarization-sensitive optical coherence tomography. *J Am Coll Cardiol* 2007;**49**:1474–1481.
20. Rekhter M. Vulnerable atherosclerotic plaque: emerging challenge for animal models. *Curr Opin Cardiol* 2002;**17**:626–632.
21. Chen J, Li D, Schaefer R, Mehta JL. Cross-talk between dyslipidemia and renin-angiotensin system and the role of LOX-1 and MAPK in atherogenesis studies with the combined use of rosuvastatin and candesartan. *Atherosclerosis* 2006;**184**:295–301.
22. Chen K, Chen J, Li D, Zhang X, Mehta JL. Angiotensin II regulation of collagen type I expression in cardiac fibroblasts: modulation by PPAR-gamma ligand pioglitazone. *Hypertension* 2004;**44**:655–661.
23. Risteli J, Risteli L. Analysing connective tissue metabolites in human serum. Biochemical, physiological and methodological aspects. *J Hepatol* 1995;**22**:77–81.
24. Becker LB. New concepts in reactive oxygen species and cardiovascular reperfusion physiology. *Cardiovasc Res* 2004;**61**:461–470.
25. Ogawa D, Stone JF, Takata Y, Blaschke F, Chu VH, Towler DA *et al.* Liver x receptor agonists inhibit cytokine-induced osteopontin expression in macrophages through interference with activator protein-1 signaling pathways. *Circ Res* 2005;**96**:e59–e67.
26. Renault MA, Jalvy S, Belloc I, Pasquet S, Sena S, Olive M *et al.* AP-1 is involved in UTP-induced osteopontin expression in arterial smooth muscle cells. *Circ Res* 2003;**93**:674–681.
27. Collins AR, Schnee J, Wang W, Kim S, Fishbein MC, Bruemmer D *et al.* Osteopontin modulates angiotensin II-induced fibrosis in the intact murine heart. *J Am Coll Cardiol* 2004;**43**:1698–1705.
28. Bruemmer D, Collins AR, Noh G, Wang W, Territo M, Arias-Magallona S *et al.* Angiotensin II-accelerated atherosclerosis and aneurysm formation is attenuated in osteopontin-deficient mice. *J Clin Invest* 2003;**112**: 1318–1331.
29. Xie Z, Singh M, Singh K. ERK1/2 and JNKs, but not p38 kinase, are involved in reactive oxygen species-mediated induction of osteopontin gene expression by angiotensin II and interleukin-1beta in adult rat cardiac fibroblasts. *J Cell Physiol* 2004;**198**:399–407.
30. Lai C-F, Seshadri V, Huang K, Shao J-S, Cai J, Vattikuti R *et al.* An osteopontin-NADPH oxidase signaling cascade promotes pro-matrix metalloproteinase 9 activation in aortic mesenchymal cells. *Circ Res* 2006;**98**:1479–1489.
31. Gorin Y, Block K, Hernandez J, Bhandari B, Wagner B, Barnes JL *et al.* Nox4 NAD(P)H oxidase mediates hypertrophy and fibronectin expression in the diabetic kidney. *J Biol Chem* 2005;**280**:39616–39626.
32. Kawashima S, Yokoyama M. Dysfunction of endothelial nitric oxide synthase and atherosclerosis. *Arterioscler Thromb Vasc Biol* 2004;**24**: 998–1005.
33. Michell BJ, Griffiths JE, Mitchelhill KI, Rodriguez-Crespo I, Tiganis T, Bozinovski S *et al.* The Akt kinase signals directly to endothelial nitric oxide synthase. *Curr Biol* 1999;**9**:845–848.
34. Colombrita C, Lombardo G, Scapagnini G, Abraham NG. Heme oxygenase-1 expression levels are cell cycle dependent. *Biochem Biophys Res Commun* 2003;**308**:1001–1008.
35. Seldon MP, Silva G, Pejanovic N, Larsen R, Gregoire IP, Filipe J *et al.* Heme oxygenase-1 inhibits the expression of adhesion molecules associated with endothelial cell activation via inhibition of NF-kappaB RelA phosphorylation at serine 276. *J Immunol* 2007;**179**:7840–7851.
36. Hoekstra KA, Godin DV, Kurtu J, Cheng KM. Effects of oxidant-induced injury on heme oxygenase and glutathione in cultured aortic endothelial cells from atherosclerosis-susceptible and -resistant Japanese quail. *Mol Cell Biochem* 2003;**254**:61–71.
37. Hsu JT, Kan WH, Hsieh CH, Choudhry MA, Schwacha MG, Bland KI *et al.* Mechanism of estrogen-mediated attenuation of hepatic injury following trauma-hemorrhage: Akt-dependent HO-1 up-regulation. *J Leukoc Biol* 2007;**82**:1019–1026.
38. Yet SF, Layne MD, Liu X, Chen YH, Ith B, Sibinga NE *et al.* Absence of heme oxygenase-1 exacerbates atherosclerotic lesion formation and vascular remodeling. *FASEB J* 2003;**17**:1759–1761.

Modulation of Angiotensin II–Mediated Hypertension and Cardiac Remodeling by Lectin-Like Oxidized Low-Density Lipoprotein Receptor-1 Deletion

Changping Hu, Abhijit Dandapat, Liuqin Sun, Muhammad R. Marwali, Nobutaka Inoue, Fumiaki Sugawara, Kazuhiko Inoue, Yosuke Kawase, Kou-ichi Jishage, Hiroshi Suzuki, Paul L. Hermonat, Tatsuya Sawamura, Jawahar L. Mehta

Abstract—Angiotensin II via type 1 receptor activation upregulates the expression of lectin-like oxidized low-density lipoprotein receptor-1 (LOX-1), and LOX-1 activation, in turn, upregulates angiotensin II type 1 receptor expression. We postulated that interruption of this positive feedback loop might attenuate the genesis of angiotensin II–induced hypertension and subsequent cardiac remodeling. To examine this postulate, LOX-1 knockout and wild-type mice were infused with angiotensin II or norepinephrine (control for angiotensin II) for 4 weeks. Angiotensin II–, but not norepinephrine-, induced hypertension was attenuated in LOX-1 knockout mice. Angiotensin II–induced cardiac remodeling was also attenuated in LOX-1 knockout mice. Importantly, angiotensin II type 1 receptor expression was reduced, and the expression and activity of endothelial NO synthase were preserved in the tissues of LOX-1 knockout mice given angiotensin II. Reactive oxygen species generation, nicotinamide-adenine dinucleotide phosphate oxidase expression, and phosphorylation of p38 and p44/42 mitogen-activated protein kinases were also much less pronounced in the LOX-1 knockout mice given angiotensin II. These alterations in biochemical and structural abnormalities were associated with preservation of cardiac hemodynamics in the LOX-1 knockout mice. To confirm that fibroblast function is modulated in the absence of LOX-1, cardiac fibroblasts from wild-type and LOX-1 knockout mice were treated with angiotensin II. Indeed, LOX-1 knockout mice cardiac fibroblasts revealed an attenuated profibrotic response on treatment with angiotensin II. These observations provide strong evidence that LOX-1 is a key modulator of the development of angiotensin II–induced hypertension and subsequent cardiac remodeling. (***Hypertension*. 2008;52:556-562.**)

Key Words: angiotensin ■ hypertension ■ cardiac remodeling ■ LOX-1 ■ oxidative stress

Cardiac remodeling is initially an adaptive response to several forms of cardiac stress states, such as hypertension. Sustained remodeling results in heart failure and is a powerful independent risk factor for cardiac morbidity and mortality.[1] Therefore, identification of the molecular mechanisms involved in cardiac remodeling is an important challenge for the cardiovascular biologists.

The renin-angiotensin system and its effector hormone, angiotensin II (Ang II), have well-known endocrine properties that contribute to cardiac remodeling and heart failure. Previous studies have shown that Ang II via type 1 receptor (AT1R) activation stimulates the expression of lectin-like oxidized low-density lipoprotein receptor-1 (LOX-1).[2] In turn, activation of LOX-1 upregulates AT1R expression.[3] Activation of both AT1R and LOX-1 induces a state of oxidative stress.[4] In addition, activation of both AT1R and LOX-1 enhances the growth of cardiac fibroblasts and promotes collagen synthesis.[5,6]

Although LOX-1 mRNA expression is minimal in normal arterial tissues, it is markedly upregulated in vascular tissues of spontaneously hypertensive animals, suggesting a correlation between LOX-1 and hypertension.[7] This concept is supported by in vitro observations that Ang II upregulates LOX-1 expression,[2] and angiotensin-converting enzyme inhibitors and AT1R blockers decrease LOX-1 expression.[8] These findings suggest that LOX-1 overexpression may contribute to the pathological states induced by Ang II. We postulated that interruption of the positive feedback loop between Ang II and LOX-1 might reduce the genesis of Ang II–induced hypertension and subsequent cardiac remodeling.

Received April 22, 2008; first decision May 12, 2008; revision accepted June 26, 2008.

From the Department of Medicine and Physiology and Biophysics (C.H., A.D., L.S., M.R.M., P.L.H., T.S., J.L.M.), University of Arkansas for Medical Sciences and Central Arkansas Veterans Healthcare System, Little Rock; Department of Pharmacology (C.H.), School of Pharmaceutical Sciences, Central South University, Changsha, China; Department of Ophthalmology (L.S.), Heping Hospital, Changzhi Medical College, Changzhi, China; Department of Vascular Physiology (N.I., F.S., K.I., T.S.), National Cardiovascular Center Research Institute, Osaka, Japan; Chugai Research Institute for Medical Science (Y.K., K-i.J.), Shizuoka, Japan; and Obihiro University of Agriculture and Veterinary Medicine (H.S.), Hokkaido, Japan.

The first 2 authors contributed equally to this work.

Correspondence to Jawahar L. Mehta, Cardiovascular Medicine, University of Arkansas for Medical Sciences, 4301 W Markham St, Slot 532, Little Rock, AR 72205-7199. E-mail MehtaJL@uams.edu

Hypertension **is available at http://hyper.ahajournals.org** **DOI: 10.1161/HYPERTENSIONAHA.108.115287**

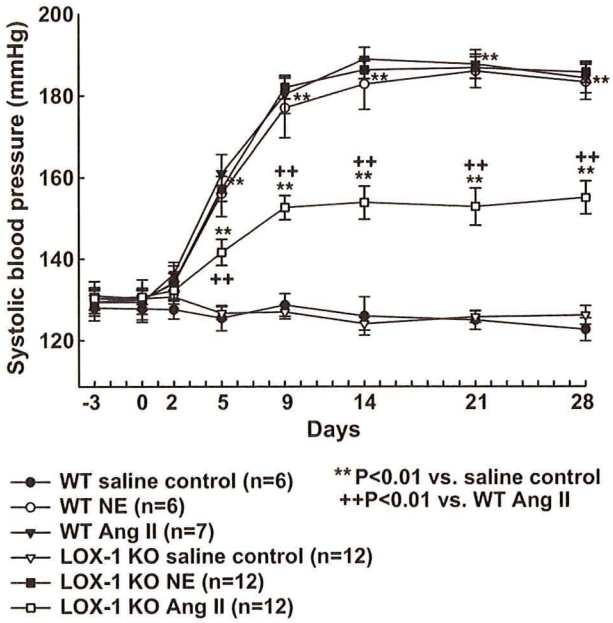

Figure 1. Systolic blood pressure rise in response to Ang II and norepinephrine (NE) infusion in wild-type (WT) and LOX-1 KO mice. LOX-1 deletion selectively attenuated blood pressure response to Ang II, but not NE, infusion.

To address this issue, we used a mouse model of LOX-1 deficiency (hereafter called LOX-1 knockout or KO mice).

Our specific aims were to examine the following hypotheses: (1) LOX-1 blockade (use of LOX-1 KO mice) will attenuate Ang II–induced hypertension; (2) cardiac remodeling after Ang II infusion will be less in the LOX-1 KO mice; and (3) fibroblasts from LOX-1 KO mice will generate less collagen (versus wild-type mice) when exposed to Ang II.

Materials and Methods

LOX-1 KO and wild-type mice were infused with Ang II (50 ng/min) or norepinephrine (100 ng/min) for 4 weeks. Blood pressure, cardiac remodeling, and oxidative stress sensitive signaling were determined. For details, please refer to the online data supplement (http://hyper.ahajournals.org). Data are expressed as means±SEs. All of the data were analyzed by a 2-way ANOVA with a Bonferroni posthoc test. A $P<0.05$ was considered significant.

Results

Blood Pressure and Cardiac Hemodynamics in Response to Ang II or Norepinephrine

Basal systolic blood pressure was similar in the wild-type and LOX-1 KO mice and remained unchanged in all of the saline-treated mice for the duration of the study. On the other hand, systolic blood pressure exhibited a progressive increase during the infusion (with Ang II or norepinephrine) period, reaching a peak value on day 14 and remaining at plateau through day 28 in the wild-type mice (Figure 1). The rise in blood pressure was much less in the LOX-1 KO mice compared with that in wild-type mice ($P<0.01$), despite infusion with the same dose of Ang II. In contrast to the effect of Ang II, norepinephrine infusion caused a similar rise in blood pressure in wild-type and LOX-1 KO mice for the duration of the study. Thus, LOX-1 deletion resulted in a selective attenuation of blood pressure in response to Ang II.

At the end of Ang II or norepinephrine infusion, we measured left ventricular hemodynamics. As shown in Figure S1, heart rate, left ventricular systolic pressure, left ventricular end-diastolic pressure, and the first derivatives of the pressure over time were similar in all of the mice, indicating that the basal hemodynamics were comparable in wild-type and LOX-1 KO mice. Ang II or norepinephrine infusion had no significant effect on heart rate in wild-type and LOX-1 KO mice but induced a marked increase in left ventricular systolic pressure, left ventricular end-diastolic pressure, and first derivatives of the pressure over time compared with corresponding saline-treated control mice ($P<0.01$). It is of note that the increase in left ventricular systolic pressure, left ventricular end-diastolic pressure, and first derivatives of the pressure over time was much less in LOX-1 KO mice compared with that in the wild-type mice despite infusion of a similar dose of Ang II ($P<0.05$). Norepinephrine-induced hemodynamic changes remained similar in wild-type and LOX-1 KO mice.

Cardiac Remodeling After Sustained Hypertension and Effect of LOX-1 Deletion

Hearts from wild-type and LOX-1 KO mice were assessed with regard to their susceptibility to hypertrophic response to sustained hypertension. Chronic Ang II, as well as norepinephrine infusion, induced significant cardiac hypertrophy (expressed as a ratio of heart weight to body weight or to tibia length) in wild-type and LOX-1 KO mice (Figure 2A through 2C; $P<0.01$ versus corresponding saline-treated mice). The cardiomyocyte cross-sectional area also increased in response to sustained hypertension (Figure 2D and 2E). Ang II–induced cardiac hypertrophy was much less in the LOX-1 KO mice compared with that in wild-type mice ($P<0.01$), as evidenced from a smaller increase in the heart weight and cross-sectional area of cardiomyocytes.

On the other hand, there was no significant difference in cardiac hypertrophy in response to norepinephrine infusion between wild-type and LOX-1 KO mice. This is in keeping with a similar degree of hypertensive response to norepinephrine in both groups of animals.

Because the increase in cardiac mass and cardiomyocyte size is accompanied by induction of specific genes, atrial natriuretic peptide (ANP) and α-tubulin,[9,10] we sought to measure their expression. As shown in Figure 3A and Figure S2, the expression of ANP and α-tubulin was increased in wild-type mice given Ang II or norepinephrine compared with saline-infused wild-type mice ($P<0.01$). Importantly, the LOX-1 KO mice demonstrated much less induction of ANP and α-tubulin despite Ang II infusion ($P<0.01$ versus Ang II–infused wild-type mice). This phenomenon was confirmed by immunohistochemical staining for α-tubulin (Figure 3B). Again, norepinephrine-induced induction of ANP and α-tubulin remained similar in wild-type and LOX-1 KO mice.

Sustained hypertension and resultant cardiac remodeling are characterized by abundant accumulation of matrix proteins in the extracellular space.[11] We, therefore, determined the accumulation of collagen in multiple sections of hearts from different animal groups. Results of Masson trichrome

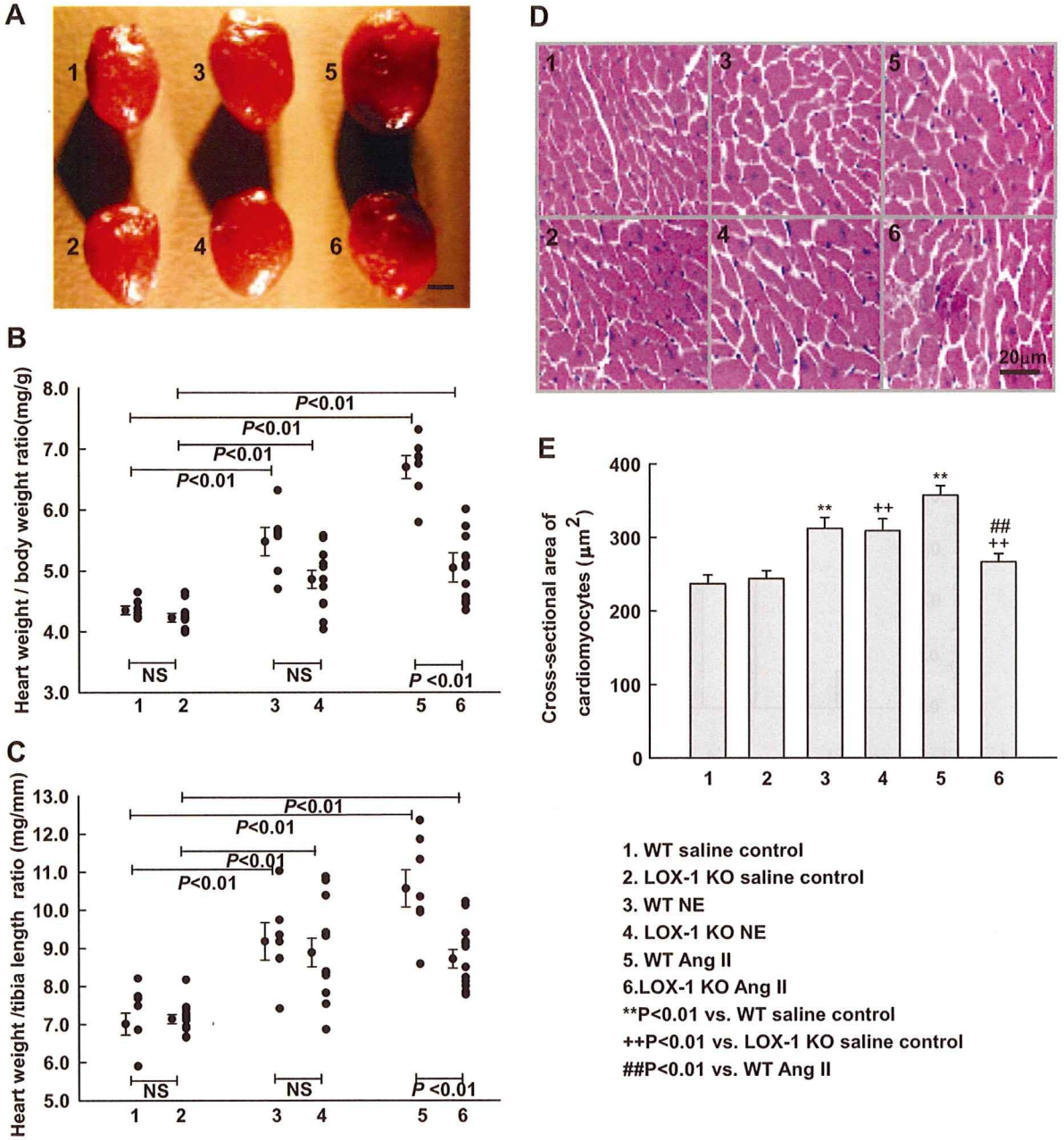

Figure 2. Cardiac hypertrophy in mice given Ang II and NE. A, Representative images of cardiac hypertrophy (bar=1 mm). B, Heart weight:body weight ratio (n=6 to 12). C, Heart weight:tibia length ratio (n=6 to 12). D, Representative images of hematoxylin-eosin micrographs of cardiomyocyte cross-sections (magnification, ×200). E, Summarized data on cardiomyocyte size (n=6). LOX-1 deletion reduced cardiac hypertrophy selectively in response to Ang II infusion.

and Picrosirius red staining were similar. Representative examples are shown in Figure 3B, and the summary data from trichrome staining are shown in Figure 3C. In the wild-type mice, sustained hypertension after Ang II or norepinephrine infusion resulted in a significant increase in collagen accumulation ($P<0.01$ versus saline-infused wild-type mice). In contrast, the LOX-1 KO mice exhibited much less increase in collagen accumulation despite Ang II infusion ($P<0.01$ versus Ang II–infused wild-type mice). Norepinephrine-induced collagen accumulation remained similar in wild-type and LOX-1 KO mice (Figure 3B and 3C).

Collagen type I, derived from its precursor procollagen I, is considered a major determinant of myocardial stiffness.[11] Osteopontin has been shown to interact with fibronectin and plays an important role in left ventricular remodeling.[12] Therefore, we determined the expression of procollagen I, osteopontin, and fibronectin in mice hearts. As shown in Figure 3A, the expression of procollagen I, osteopontin, and fibronectin increased significantly after infusion of Ang II or norepinephrine in the wild-type mice ($P<0.01$ versus saline-infused wild-type mice). However, LOX-1 KO mice given Ang II infusion exhibited much less increase in the expression of procollagen I, osteopontin, and fibronectin in the LOX-1 KO mice ($P<0.01$ versus wild-type mice). The expression of procollagen I, osteopontin, and fibronectin induced by norepinephrine infusion was similar in wild-type

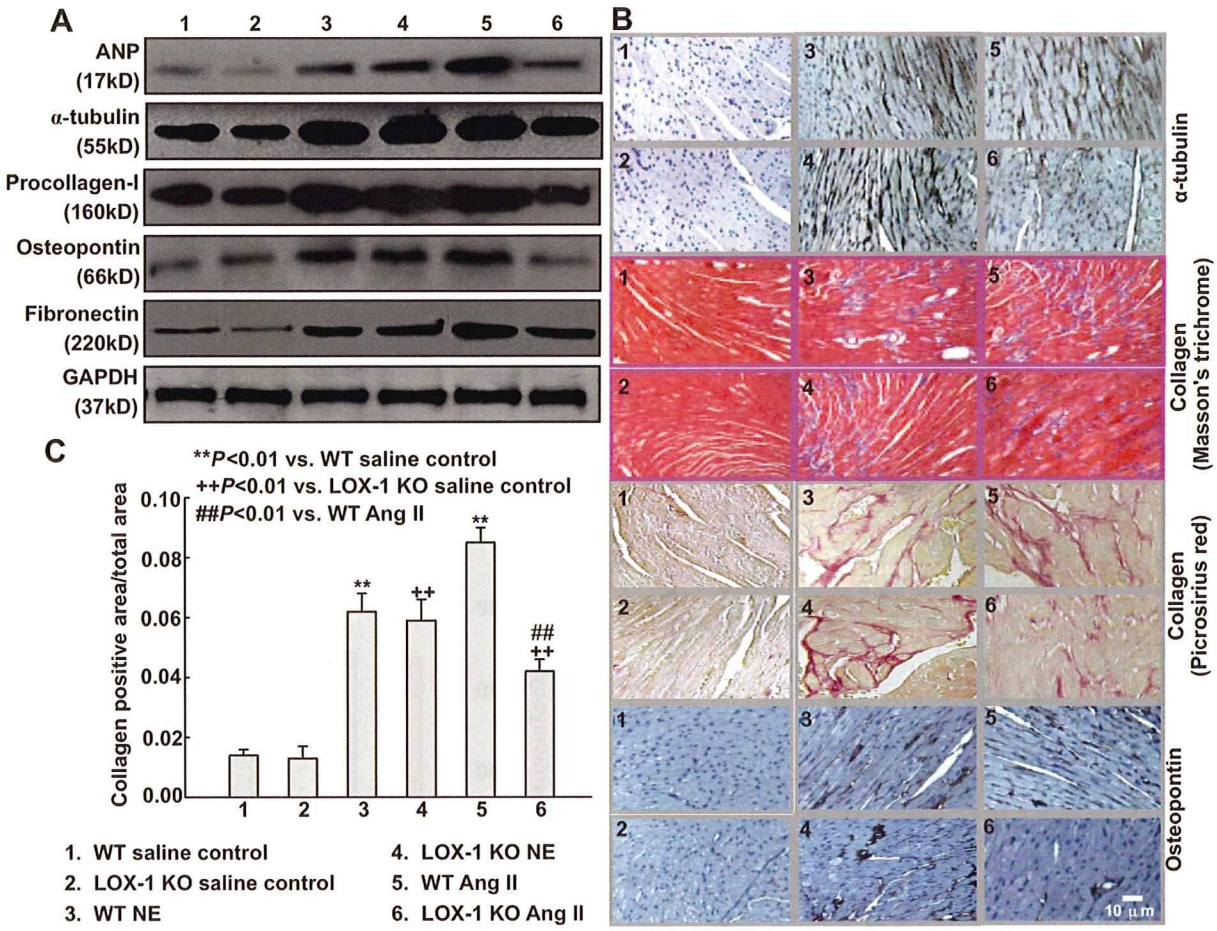

Figure 3. Markers of cardiac hypertrophy (ANP and α-tubulin) and fibrosis (collagen, procollagen-I, osteopontin, and fibronectin) in mice given Ang II and NE. A, Representative Western blot. B, Immunostaining of α-tubulin, collagen, and osteopontin. C, Summary of data on trichrome staining. These markers of cardiac remodeling were less pronounced in LOX-1 KO mice given Ang II. Data are representative of 4 experiments.

and LOX-1 KO mice. We also performed immunohistochemical staining for osteopontin in heart sections, and the data were consistent with the results by Western analysis (Figure 3B).

Expression of AT1R and Endothelial NO Synthase Induced by Ang II Infusion and the Effect of LOX-1 Deletion

Most of the cardiovascular actions of Ang II have been attributed to AT1R activation, whereas the hypertensive response to norepinephrine is related to α_1-adrenoceptor activation.[13,14] We, therefore, determined the expression of AT1R and α_1-adrenoceptors. As shown in Figure 4A and Figure S3, AT1R expression increased in the aortic and cardiac tissues after infusion of Ang II in the wild-type mice ($P<0.01$ versus saline-infused wild-type mice). However, Ang II-infused LOX-1 KO mice exhibited much less increase in AT1R expression ($P<0.01$ versus wild-type mice). Interestingly, the expression of α_1-adrenceptors induced by norepinephrine infusion remained similar in aortic and cardiac tissues from wild-type and LOX-1 KO mice (Figure 4B).

Our recent study has shown that endothelium-dependent relaxation of aorta, as well as endothelial NO synthase (eNOS) expression, is preserved in the LOX-1 KO mice fed a high-cholesterol diet.[15] In the present study, we measured the expression of eNOS and phosphorylated S1177-eNOS in the aorta and found that wild-type mice given Ang II had low levels of eNOS and phosphorylated S1177-eNOS ($P<0.01$ versus control mice). Importantly, LOX-1 deletion preserved the expression of eNOS and phosphorylated S1177-eNOS despite Ang II infusion ($P<0.01$; Figure 4C). It is of note that the downregulation of eNOS and phosphorylated eNOS expression induced by norepinephrine infusion remained similar in aortas from wild-type and LOX-1 KO mice (Figure 4C).

Oxidative Stress Induced by Ang II and Norepinephrine and the Effect of LOX-1 Deletion

Oxidative stress and resultant release of reactive oxygen species (ROS) have been linked to the development of cardiac remodeling and progression to heart failure.[16] Ang II also upregulates LOX-1 expression.[2] Therefore, we determined nicotinamide-adenine dinucleotide phosphate (NADPH) oxidase ($p47^{phox}$ and $p22^{phox}$ subunits) expression, ROS production, phosphorylation of oxidative stress–sensitive mitogen-activated protein kinases (MAPKs; p38 and p44/42 MAPK isoforms), and LOX-1 expression. In keeping with previous in vitro studies,[17] Ang II infusion induced oxidative stress (dichlorofluorescein fluorescence, 8-isoprostane in hearts, serum malondialdehyde, and $p47^{phox}$

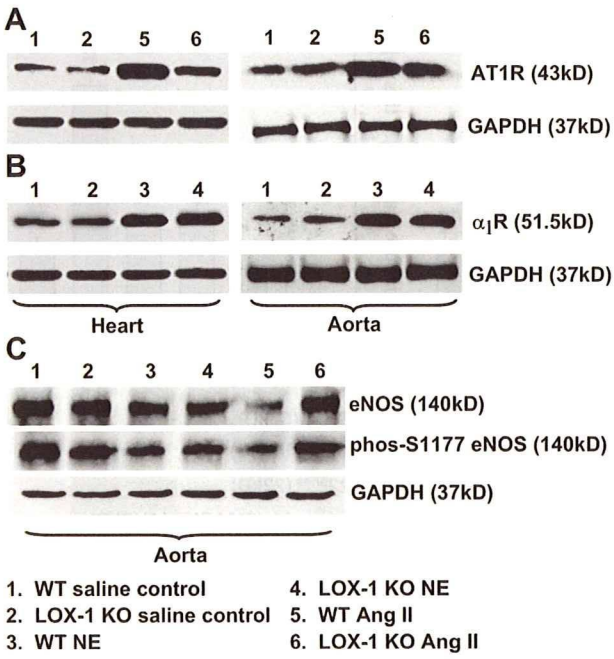

Figure 4. Expression of AT1R, α_1-adrenoceptor (α1R), and eNOS in mice given Ang II and norepinephrine (NE). LOX-1 deletion caused attenuation of AT1R expression and enhancement of eNOS expression/activity in response to Ang II. The expression of α1R and eNOS in response to NE was not affected by LOX-1 deletion.

and p22^{phox} subunits, Figure 5A through 5D) in the wild-type mice, but much less so in the LOX-1 KO mice. Norepinephrine infusion also increased oxidative stress in the wild-type mice, but it was not affected by LOX-1 deletion.

As shown in Figure 5D and Figure S4, protein levels of p38 and p44/42 MAPKs were unchanged in response to Ang II and norepinephrine infusion, but their phosphorylation increased significantly during Ang II infusion ($P<0.01$ versus saline-infused wild-type mice). Importantly, Ang II-infused LOX-1 KO mice exhibited much less phosphorylation of MAPKs ($P<0.01$ versus Ang II–infused wild-type mice). However, the increased phosphorylation of MAPKs during norepinephrine infusion was not affected by LOX-1 deletion.

In keeping with previous in vitro studies,[2] Ang II infusion enhanced LOX-1 expression in the wild-type mice (Figure 5D). As expected, LOX-1 was not detectable in LOX-1 KO mice hearts. Importantly, LOX-1 expression was only minimally upregulated by norepinephrine infusion.

Studies in Cultured Cardiac Fibroblasts

Fibroblasts form a significant component of cardiac mass, and their growth and activity (collagen formation) contribute to cardiac remodeling.[5,6,11] To mimic the in vivo state, we treated mouse cardiac fibroblasts with Ang II (1 μmol/L) for 24 hours. Prolonged exposure of cardiac fibroblasts from wild-type mice to Ang II induced dichlorofluorescein fluorescence and NADPH oxidase (p47^{phox} and p22^{phox} subunits) expression, but these changes were much less pronounced in fibroblasts from LOX-1 KO mice despite their treatment with Ang II ($P<0.01$). In addition, phosphorylation of p38 and p44/42 MAPK, which was quite marked in the fibroblasts from wild-type mice, was less in fibroblasts from LOX-1 KO mice despite their exposure to Ang II (Figure S5).

Treatment with Ang II for 24 hours also increased procollagen I expression in cardiac fibroblasts from wild-type mice, but to a much smaller extent in fibroblasts from LOX-1 KO mice (Figure S6). These data are consistent with the data on collagen staining in the hearts from wild-type and LOX-1 KO mice. LOX-1 expression was also quite marked in cardiac fibroblasts isolated from wild-type mice. As expected, fibroblasts isolated from LOX-1 KO mice showed the absence of LOX-1 (Figure S6).

Discussion

We show that LOX-1 deletion attenuated Ang II–induced hypertension and cardiac remodeling. Most importantly, our in vitro studies confirmed that fibroblasts from LOX-1 KO mice generated much less collagen (versus wild-type mice) when exposed to Ang II.

Ang II via AT1R activation upregulates LOX-1 through redox-sensitive pathways,[18] and activation of LOX-1 upregulates AT1R expression.[3] We, accordingly, postulated that Ang II and LOX-1 operate in a positive feedback fashion with the common theme being generation of ROS and activation of MAPKs. To examine the relevance of this postulate in the in vivo state, we measured blood pressure response to Ang II in wild-type mice and studied the role of LOX-1 abrogation by using the LOX-1 KO mice. In these LOX-1 KO mice, endothelium-dependent relaxation, as well as eNOS generation, is preserved when the animals are fed a high-cholesterol diet.[15] In the present study, we observed that, whereas the resting blood pressure was similar in the LOX-1 KO and wild-type mice, blood pressure rise in response to Ang II was markedly attenuated in the LOX-1 KO mice. Interestingly, AT1R expression increased in the wild-type mice given Ang II infusion, as observed by others as well.[19] The expression and activity of eNOS both decreased in the wild-type mice given Ang II. Importantly, the LOX-1 KO mice given Ang II infusion exhibited a much smaller increase in the expression of AT1R and a marked upregulation of eNOS expression/activity compared with the wild-type mice. These findings confirm that the Ang II-AT1R-LOX-1 loop is an important regulator of blood pressure.

The blood pressure increase in response to norepinephrine was not affected by LOX-1 abrogation. It is of note that norepinephrine infusion caused only a minimal change in LOX-1 expression (versus a large increase in Ang II–infused mice). Norepinephrine infusion, as expected, increased α_1-adrenoceptor expression, and LOX-1 deletion did not affect α_1-adrenoceptor upregulation. LOX-1 deletion also had no effect on the downregulation of eNOS expression/activity induced by norepinephrine infusion. As such, it is not surprising that the norepinephrine-α_1-adrenoceptor-hypertension pathway was not affected by LOX-1 deletion. Many studies have shown that Ang II causes ROS generation by activating NADPH oxidases,[16,17] which, in turn, activate p38 and/or p44/42 MAPKs and redox-sensitive transcription factors.[17] This process influences downstream signals, resulting in cardiomyocyte hypertrophy and procollagen synthesis.[11,16,17] Activation of this cascade has been thought to lead

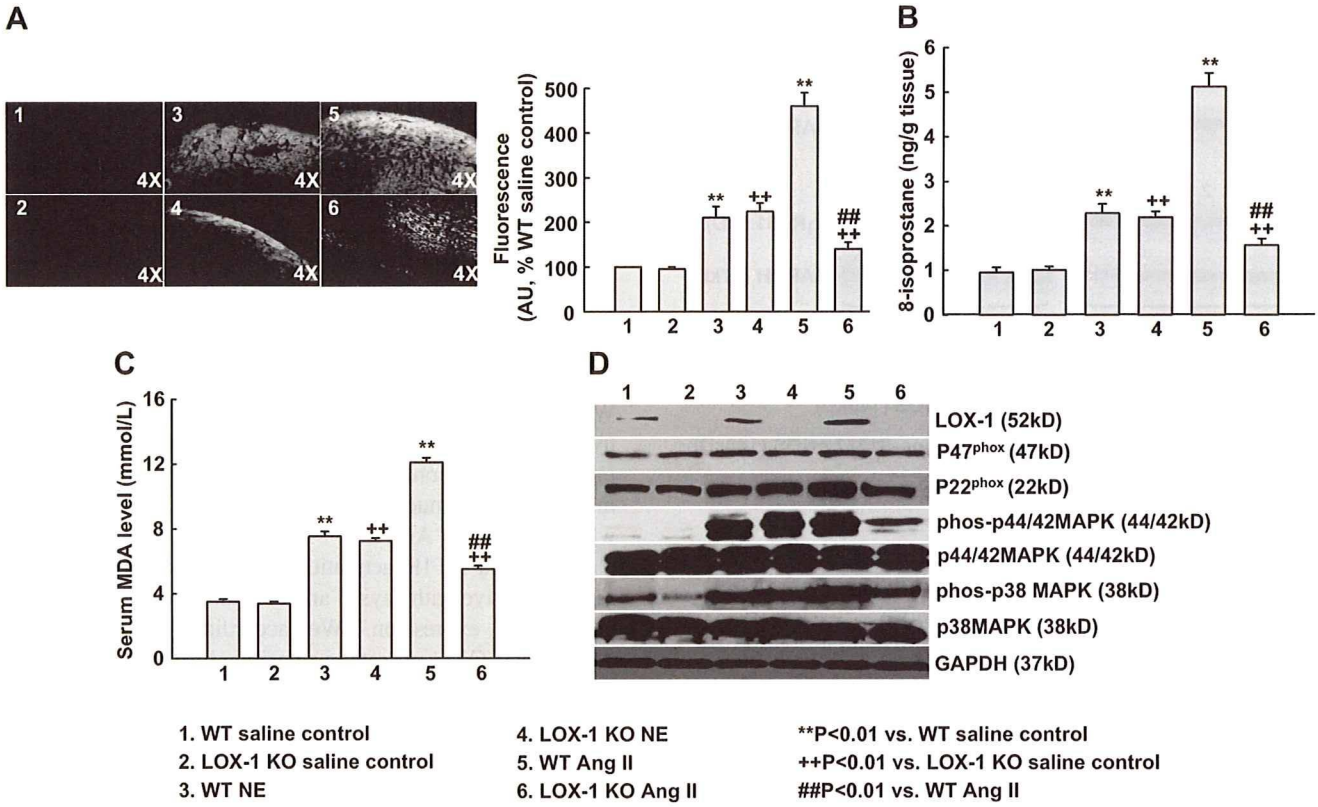

Figure 5. Oxidative stress and LOX-1 expression in mice given Ang II or NE. A, Representative dichlorofluorescein fluorescence images indicating reactive oxygen species release in heart and the summary of fluorescence data (n=5). B, Cardiac 8-isoprostane level (n=5). C, Serum malondialdehyde (MDA) levels (n=5). Note the marked dichlorofluorescein fluorescence in Ang II–infused wild-type (WT) mice heart; the fluorescence was attenuated in LOX-1 KO mice hearts. Norepinephrine (NE) infusion caused much less fluorescence (vs Ang II infusion), and LOX-1 deletion had no effect. D, Representative Western blots. Ang II, but not NE, infusion increased LOX-1 expression in WT mice. Both NE and Ang II enhanced phosphorylation of p38 and p44/42 MAPKs in WT mice. LOX-1 deletion reduced phosphorylation of MAPKs selectively in response to Ang II but not NE. This Western blot is representative of 4 separate experiments.

to the development of cardiac remodeling in sustained hypertension.[16] This concept is supported by the observations that the NADPH oxidase inhibitor apocynin reduces blood pressure elevation and prevents vascular remodeling in Ang II–infused mice. Furthermore, hydralazine, which decreases blood pressure but does not affect ROS and related pathways, has no effects on vascular remodeling induced by Ang II.[20]

We observed that prolonged infusion of Ang II, as well as norepinephrine, increased heart weight in the wild-type mice. The increase in heart weight was a manifestation of cardiomyocyte hypertrophy, because cardiomyocyte cross-sectional area and α-tubulin and ANP expression in the heart were enhanced. In addition, there was clear evidence of fibroblast proliferation and collagen accumulation. It is worth noting that the cardiomyocyte hypertrophy and fibrosis were greater in Ang II–infused mice as compared with norepinephrine-infused mice, perhaps an indication of greater ROS generation in response to Ang II despite a similar degree of blood pressure elevation (Figure 1). Ang II–infused LOX-1 KO mice exhibited a very low level of ROS generation and downstream signal activation. It was, therefore, not surprising that LOX-1 KO mice had much less cardiomyocyte hypertrophy and collagen deposition (versus the wild-type mice) despite infusion of same doses of Ang II. The LOX-1 KO mice given norepinephrine infusion did not exhibit any significant changes in ROS generation and downstream signaling, and, hence, showed no change in cardiomyocyte hypertrophy and fibrosis. Previous studies have demonstrated that LOX-1 is a key modulator of cardiac remodeling, which starts immediately after a brief period of ischemia reperfusion via ROS-dependent pathways, and that the signals of cardiac remodeling are attenuated in the LOX-1 KO mice.[21]

We also found that the expression of osteopontin, as well as fibronectin, increased in the wild-type mice given Ang II and norepinephrine. Osteopontin has been shown to interact with fibronectin and plays an important role in matrix organization and stability.[12] Previous studies also showed that Ang II increases osteopontin expression, and the osteopontin null mice given Ang II infusion have much less cardiac fibrosis and hypertrophy.[22,23] Xie et al[24] showed that the signals for Ang II–induced osteopontin expression also involve oxidative stress and resultant p42/44 MAPK activation. Gorin et al[25] have similarly shown a relationship between NADPH oxidase activation and fibronectin generation both in vitro and in vivo. In keeping with these studies, we found that the expression of procollagen I, as well as osteopontin and fibronectin, was lower in the hearts of Ang II–treated LOX-1 KO mice that had low levels of oxidant stress and activation of MAPKs.

The data on cultured cardiac fibroblasts exposed to Ang II in vitro support the in vivo observations in mice given Ang II

infusion. The fibroblasts from LOX-1 KO mice revealed much less oxidative stress and activation of MAPKs compared with fibroblasts from wild-type mice after exposure to Ang II. In keeping with previous studies in rodent cardiac fibroblasts,[5,17] Ang II exposure induced procollagen I expression, but the procollagen I expression was decreased by LOX deletion. Chen et al[6] showed that the overexpression of LOX-1 in rat cardiac fibroblasts enhances the expression of collagen I and the phosphorylation of p38 MAPK. These observations further suggest that the Ang II (AT1R)-ROS-LOX-1 loop might directly regulate the development of cardiac remodeling in mice with an Ang II–induced increase in blood pressure.

Perspectives

This study provides exciting in vivo evidence of a positive feedback loop between Ang II-ROS-LOX-1, which results in the syndrome of chronic sustained hypertension, and cardiac remodeling. The in vitro component using cardiac fibroblasts from LOX-1 KO and wild-type mice lends support to this concept. Our study does not allow us to dissociate the direct effect of LOX-1 deletion on cardiac hypertrophy from its blood pressure–attenuating effects. Therefore, the role of LOX-1 in the regulation of cardiac remodeling needs to be further investigated in other models of pressure or volume overload or in primary cultured cardiomyocytes.

Sources of Funding

This study was supported by funds from the Department of Veterans Affairs (J.L.M.) and a grant from the American Heart Association (P.L.H.); the Ministry of Education, Culture, Sports, Science, and Technology of Japan (T.S.); the Ministry of Health, Labor, and Welfare of Japan (T.S.); and the National Institute of Biomedical Innovation, Japan (T.S.).

Disclosures

None.

References

1. Hilfiker-Kleiner D, Landmesser U, Drexler H. Molecular mechanisms in heart failure. Focus on cardiac hypertrophy, inflammation, angiogenesis, and apoptosis. *J Am Coll Cardiol*. 2006;48:A56–A66.
2. Chen J, Liu Y, Liu H, Hermonat PL, Mehta JL. Molecular dissection of angiotensin II-activated human LOX-1 promoter. *Arterioscler Thromb Vasc Biol*. 2006;26:1163–1168.
3. Li D, Saldeen T, Romeo F, Mehta JL. Oxidized LDL upregulates angiotensin II type 1 receptor expression in cultured human coronary artery endothelial cells: the potential role of transcription factor NF-kappaB. *Circulation*. 2000;102:1970–1976.
4. Mehta JL, Chen J, Hermonat PL, Romeo F, Novelli G. Lectin-like, oxidized low-density lipoprotein receptor-1 (LOX-1): a critical player in the development of atherosclerosis and related disorders. *Cardiovasc Res*. 2006;69:36–45.
5. Chen K, Mehta JL, Li D, Joseph L, Joseph J. Transforming growth factor beta receptor endoglin is expressed in cardiac fibroblasts and modulates profibrogenic actions of angiotensin II. *Circ Res*. 2004;95:1167–1173.
6. Chen K, Chen J, Liu Y, Xie J, Li D, Sawamura T, Hermonat PL, Mehta JL. Adhesion molecule expression in fibroblasts: alteration in fibroblast biology after transfection with LOX-1 plasmids. *Hypertension*. 2005;46:622–627.
7. Nagase M, Hirose S, Sawamura T, Masaki T, Fujita T. Enhanced expression of endothelial oxidized low-density lipoprotein receptor (LOX-1) in hypertensive rats. *Biochem Biophys Res Commun*. 1997;237:496–498.
8. Morawietz H, Rueckschloss U, Niemann B, Duerrschmidt N, Galle J, Hakim K, Zerkowski HR, Sawamura T, Holtz J. Angiotensin II induces LOX-1, the human endothelial receptor for oxidized low-density lipoprotein. *Circulation*. 1999;100:899–902.
9. Arimoto T, Takeishi Y, Takahashi H, Shishido T, Niizeki T, Koyama Y, Shiga R, Nozaki N, Nakajima O, Nishimaru K, Abe J, Endoh M, Walsh RA, Goto K, Kubota I. Cardiac-specific overexpression of diacylglycerol kinase zeta prevents Gq protein-coupled receptor agonist-induced cardiac hypertrophy in transgenic mice. *Circulation*. 2006;113:60–66.
10. Kee HJ, Sohn IS, Nam KI, Park JE, Qian YR, Yin Z, Ahn Y, Jeong MH, Bang YJ, Kim N, Kim JK, Kim KK, Epstein JA, Kook H. Inhibition of histone deacetylation blocks cardiac hypertrophy induced by angiotensin II infusion and aortic banding. *Circulation*. 2006;113:51–59.
11. Weber KT. Fibrosis, a common pathway to organ failure: angiotensin II and tissue repair. *Semin Nephrol*. 1997;17:467–491.
12. Kossmehl P, Schonberger J, Shakibaei M, Faramarzi S, Kurth E, Habighorst B, von Bauer R, Wehland M, Kreutz R, Infanger M, Schulze-Tanzil G, Paul M, Grimm D. Increase of fibronectin and osteopontin in porcine hearts following ischemia and reperfusion. *J Mol Med*. 2005;83:626–637.
13. Weiss D, Kools JJ, Taylor WR. Angiotensin II-induced hypertension accelerates the development of atherosclerosis in apoE-deficient mice. *Circulation*. 2001;103:448–454.
14. Cervenka L, Maly J, Karasova L, Simova M, Vitko S, Hellerova S, Heller J, El-Dahr SS. Angiotensin II-induced hypertension in bradykinin B2 receptor knockout mice. *Hypertension*. 2001;37:967–973.
15. Mehta JL, Sanada N, Hu CP, Chen J, Dandapat A, Sugawara F, Takeya M, Inoue K, Kawase Y, Jishage KI, Suzuki H, Satoh H, Schnackenberg L, Beger R, Hermonat PL, Thomas M, Sawamura T. Deletion of LOX-1 reduces atherogenesis in LDLR knockout mice fed high cholesterol diet. *Circ Res*. 2007;100:1634–1642.
16. Sorescu D, Griendling KK. Reactive oxygen species, mitochondria, and NAD(P)H oxidases in the development and progression of heart failure. *Congest Heart Fail*. 2002;8:132–140.
17. Chen J, Mehta JL. Angiotensin II-mediated oxidative stress and procollagen-1 expression in cardiac fibroblasts: blockade by pravastatin and pioglitazone. *Am J Physiol Heart Circ Physiol*. 2006;291:H1738–H1745.
18. Li D, Zhang YC, Philips MI, Sawamura T, Mehta JL. Upregulation of endothelial receptor for oxidized low-density lipoprotein (LOX-1) in cultured human coronary artery endothelial cells by angiotensin II type 1 receptor activation. *Circ Res*. 1999;84:1043–1049.
19. Harrison-Bernard LM, El-Dahr SS, O'Leary DF, Navar LG. Regulation of angiotensin II type 1 receptor mRNA and protein in angiotensin II-induced hypertension. *Hypertension*. 1999;33:340–346.
20. Virdis A, Neves MF, Amiri F, Touyz RM, Schiffrin EL. Role of NAD(P)H oxidase on vascular alterations in angiotensin II-infused mice. *J Hypertens*. 2004;22:535–542.
21. Hu CP, Dandapat A, Chen J, Fujita Y, Inoue N, Kawase Y, Jishage K, Suzuki H, Sawamura T, Mehta JL. LOX-1 deletion alters signals of myocardial remodeling immediately after ischemia-reperfusion. *Cardiovascular Res*. 2007;76:292–302.
22. Matsui Y, Jia N, Okamoto H, Kon S, Onozuka H, Akino M, Liu L, Morimoto J, Rittling SR, Denhardt D, Kitabatake A, Uede T. Role of osteopontin in cardiac fibrosis and remodeling in angiotensin II-induced cardiac hypertrophy. *Hypertension*. 2004;43:1195–1201.
23. Collins AR, Schnee J, Wang W, Kim S, Fishbein MC, Bruemmer D, Law RE, Nicholas S, Ross RS, Hsueh WA. Osteopontin modulates angiotensin II-induced fibrosis in the intact murine heart. *J Am Coll Cardiol*. 2004;43:1698–1705.
24. Xie Z, Singh M, Singh K. ERK1/2 and JNKs, but not p38 kinase, are involved in reactive oxygen species-mediated induction of osteopontin gene expression by angiotensin II and interleukin-1beta in adult rat cardiac fibroblasts. *J Cell Physiol*. 2004;198:399–407.
25. Gorin Y, Block K, Hernandez J, Bhandari B, Wagner B, Barnes JL, Abboud HE. Nox4 NAD(P)H oxidase mediates hypertrophy and fibronectin expression in the diabetic kidney. *J Biol Chem*. 2005;280:39616–39626.

Importance of Forkhead Transcription Factor Fkhl18 for Development of Testicular Vasculature

YUKO SATO,[1] TAKASHI BABA,[1] MOHAMAD ZUBAIR,[1] KANAKO MIYABAYASHI,[1] YOSHIRO TOYAMA,[2] MAMIKO MAEKAWA,[2] AKIKO OWAKI,[1] HIROFUMI MIZUSAKI,[1] TATSUYA SAWAMURA,[3] KIYOTAKA TOSHIMORI,[2] KEN-ICHIROU MOROHASHI,[1]* AND YUKO KATOH-FUKUI[1]

[1]*Division of Sex Differentiation, National Institute for Basic Biology, National Institutes of Natural Sciences, Okazaki, Japan*

[2]*Department of Anatomy, Graduate School of Medicine, Chiba University, Chiba, Japan*

[3]*Department of Vascular Physiology, National Cardiovascular Center Research Institute, Suita, Osaka, Japan*

ABSTRACT Forkhead transcription factors are characterized by a winged helix DNA binding domain, and the members of this family are classified into 20 subclasses by phylogenetic analyses. *Fkhl18* is structurally unique, and is classified into FoxS subfamily. We found *Fkhl18* expression in periendothelial cells of the developing mouse fetal testis. In an attempt to clarify its function, we generated mice with *Fkhl18* gene disruption. Although KO mice developed normally and were fertile in both sexes, we frequently noticed unusual blood accumulation in the fetal testis. Electron microscopic analysis demonstrated frequent gaps, measuring 100–400 nm, in endothelial cells of blood vessels. These gaps probably represented ectopic apoptosis of testicular periendothelial cells, identified by caspase-3 expression, in KO fetuses. No apoptosis of endothelial cells was noted. Fkhl18 suppressed the transcriptional activity of FoxO3a and FoxO4. Considering that *Fas ligand* gene expression is activated by Foxs, the elevated activity of Foxs in the absence of *Fkhl18* probably explains the marked apoptosis of periendothelial cells in *Fkhl18* KO mice. *Mol. Reprod. Dev.*

Key Words: forkhead; *Fkhl18*; gonad; periendothelial cells; endothelial cells; angiogenesis; vasculogenesis; fetal development

INTRODUCTION

There is a general agreement that gonad sex determination in mammals is a process initiated by *Sry* gene (sex-determining region of the Y chromosome; Koopman et al., 1990; Sinclair et al., 1990; Brennan and Capel, 2004). Downstream of *Sry*, *Sox9* (Sry-related HMG-box gene 9) specifies Sertoli cell lineages, organization of the testicular cord, and production of male hormones. In addition, the vasculature system develops differentially between the testis and ovary. Before the actions of *Sry* are evoked at around embryonic day 11.0 (E11.0), the structure of the primitive vasculature in the genital ridge is similar irrespective of sex. However, during the early phase of gonad sex differentiation, the mesonephric cells migrate vigorously into the developing testis to form a vasculature structure characteristic for the testis (Buehr et al., 1993; Martineau et al., 1997; Capel et al., 1999; Brennan et al., 2002, 2003). In contrast, no such active cell migration is observed in the developing fetal ovary. This difference gives rise to sexually dimorphic vascular patterns of the gonads. Particularly, in the testis, a large artery is formed at the coelomic surface at around E12.5. This male-specific vascular system that develops during fetal life is thought to be required for export of testosterone from the testis to the rest of the fetus to ensure masculinization (Renfree et al., 1995).

Vasculogenesis starts during fetal development. Precursor cells for blood vessel endothelia, which share origin with hematopoietic progenitors, assemble into a primitive vascular network of small capillaries. Subsequently, the vascular plexus progressively expands by sprouting and matures into stable blood vessels. During this phase of angiogenesis and arteriogenesis, nascent endothelial cells become covered by periendothelial cells

Grant sponsor: Ministry of Education, Culture, Sports Science, and Technology of Japan; Grant sponsor: Japan Science and Technology Corporation.

Yuko Sato's present address is Department of Vascular Physiology, National Cardiovascular Center Research Institute, Suita, Osaka 565-8565, Japan.

Mohamad Zubair's present address is Departments of Internal Medicine and Pharmacology, UT Southwestern Medical Center, Dallas, Texas 75390.

Hirofumi Mizusaki's present address is Department of Biochemistry, Nagasaki University School of Medicine, Nagasaki 852-8523, Japan.

Ken-Ichirou Morohashi's present address is Department of Molecular Biology, Graduate School of Medical Sciences, Kyushu University, Maidashi3-1-1, Higashi-Ku, Fukuoka 812-8582, Japan.

Yuko Katoh-Fukui's present address is Department of Aging Intervention, National Institute for Longevity Science, National Center for Geriatrics and Gerontology, Obu 474-8511, Japan.

*Correspondence to: Ken-Ichirou Morohashi, PhD, Division of Sex Differentiation, National Institute for Basic Biology, National Institutes of Natural Sciences, 5-1 Higashiyama, Myodaiji, Okazaki 444-8787, Japan. E-mail: moro@nibb.ac.jp

Received 2 December 2007; Accepted 18 December 2007
Published online in Wiley InterScience (www.interscience.wiley.com).
DOI 10.1002/mrd.20888

(pericytes and smooth muscle cells) and association with these cells is required to regulate proliferation, survival, migration, differentiation, vascular branching, blood flow, and vascular permeability (Carmeliet, 2003, 2005).

Forkhead (Fox) transcription factors carry a winged helix DNA-binding domain that share homology with their founding member forkhead protein in *Drosophila*. Phylogenic analysis of the forkhead domain consisting of highly conserved 100 amino acids led to placement of the family members into 20 subclasses, *FoxA* to *FoxS*. Foxs bind to consensus sequences, RYMAAYA (R = A or G; Y = C or T; M = A or C), as a monomer. Regions other than the conserved domain vary in terms of sequence and function. Some members act as transcriptional activators while others as repressors. Probably as transcriptional regulators, *Fox* genes are thought to play a variety of roles in fetal and adult tissues. In fact, gene knockout studies demonstrated that *Foxa2* is required for node and notochord formation, gastrulation, neural tube patterning, and gut morphogenesis (Ang and Rossant, 1994), *Foxi1/Fkh10* for inner ear development (Hulander et al., 1998, 2003), *Foxb1/Mf3* for the development of the diencephalon and midbrain, postnatal growth, and the milk-ejection reflex (Labosky et al., 1997), and *Foxc2/MFH1* for proliferation and patterning of paraxial mesoderm (Winnier et al., 1997).

Mutations in *FOX* genes have been linked to human diseases. Mutation of *FOXC1*, *FOXC2*, *FOXE1*, *FOXE3*, *FOXL2*, *FOXN1*, *FOXP2*, and *FOXP3* genes have been detected in various human congenital disorders (Mears et al., 1998; Frank et al., 1999; Chatila et al., 2000; Crisponi et al., 2001; Erickson et al., 2001; Lai et al., 2001; Semina et al., 2001; Brice et al., 2002; Castanet et al., 2002; Harris et al., 2002). Moreover, disordered expressions and functions of *FOX* genes were reported to correlate with carcinogenesis. For example, *FOXA1* gene is amplified and overexpressed in not all but certain esophageal and lung cancers (Lin et al., 2002). Likewise, in pancreatic cancer and basal cell carcinoma, *FOXM1* gene is upregulated due to transcriptional regulation by the Sonic Hedgehog (SHH) pathway (Teh et al., 2002). *FOXO1* gene is fused to *PAX3* or *PAX7* gene in rhabdomyosarcoma (Galili et al., 1993; Sorensen et al., 2002), while *FOXO3* and *FOXO4* genes are fused to myeloid/lymphoid or mixed-lineage leukemia (*MLL*) gene in hematological malignancies (Parry et al., 1994; Hillion et al., 1997). Several other studies demonstrated that these proteins are components of different signal transduction pathways, including those downstream of insulin, activin, and other transforming growth factor β-related ligands (Chen et al., 1996, 1997; Ogg et al., 1997; Nakae et al., 2002; Accili and Arden, 2004).

Fkhl18, a member of the *Fox* family, was originally identified by low-stringency screening of mouse (Kaestner et al., 1993) and human (Pierrou et al., 1994) genomic libraries. *Fkhl18* has low homology to other members of the Fox family, and is categorized under the *FoxS* subclass. However, its expression and function remain to be examined. In the present study, we demonstrated that *Fkhl18* is expressed in periendothelial cells and Sertoli cells of the developing fetal testis. We then generated the *Fkhl18*-deficient mouse to examine the physiological function of the gene product. Interestingly, the KO fetuses displayed affected testicular vasculature, suggesting that *Fkhl18* is involved in development of the fetal testis vasculature system.

MATERIALS AND METHODS

Reverse Transcription-Polymerase Chain Reaction (RT-PCR)

Total RNAs prepared from E16.5 fetal gonads were reverse-transcribed with Superscript II RNase H$^-$ Reverse Transcriptase (Invitrogen, San Diego, CA). PCR (94°C for 15 sec, 65°C for 30 sec, 68°C for 1 min, 30 cycles) was performed using the following primers for *Fkhl18* (NM_010226), Fkhl18-P1 (5′-CCC ACC AAG CCC CCT TAC AGC-3′) and Fkhl18-P2 (5′-GTC TGC GGC GAC GGA GAA AGC-3′), and for β-actin, β-actin-5′ (5′-ATG GAT GAC GAT ATC GCT-3′) and β-actin-3′ (5′-ATG GGT AGT CTG TCA GGT-3′).

In Situ Hybridization and Immunohistochemistry

E14.5 fetuses were fixed with 4% paraformaldehyde (PFA) at 4°C overnight and immersed in 30% sucrose. The fetuses were embedded in OCT compound and cryosectioned at 10 μm. The sections were treated with 1 mg/ml proteinase K (Merck, Tokyo, Japan) for 10 min at room temperature, acetylated and hybridized with 50 ng/ml riboprobe in 50% formamide, 5× SSC, 5 mM ethylenediaminetetraacetic acid (EDTA), 0.1% 3-[(3-cholamidopropyl) dimethylammonio]-1-propane sulfonate (CHAPS), 0.1% Tween-20, 0.2 mg/ml yeast tRNA, 0.1 mg/ml heparin sodium, and 1× Denhardt's solution, at 65°C. Thereafter, the sections were washed with 1× SSC containing 50% formaldehyde 30 min at 65°C. Digoxigenin (DIG)-labeled riboprobe (Roche Diagnostics, Mannheim, Germany) for full-length cDNA of *Fkhl18* was used. The DIG probes were visualized by alkaline phosphatase-conjugated anti-DIG antibody and NBT/BCIP reaction (Roche). Subsequently, some of the above sections were further subjected to immunohistochemistry using anti-*Ad4BP/SF-1* as described previously (Morohashi et al., 1994).

For immunohistochemistry, frozen sections were prepared from PFA-fixed E14.5 fetuses. The sections were dried and washed in phosphate buffered saline (PBS). After blocking with 2% skim milk for 30 min at room temperature, the sections were incubated overnight with rabbit anti-active-type caspase3 (BD Pharmingen, San Diego, CA, 1:50), rat anti-PECAM (BD Pharmingen, 1:500), or rabbit anti-β-galactosidase antibody at 4°C. The immunoreaction was detected using fluorophore conjugated secondary antibodies (Invitrogen). Nuclei were counterstained with 4′,6-diamidino-2-phenylindole (DAPI) (Sigma Chemical Co., St. Louis, MO). For double immunohistochemistry with rat anti-PECAM and

rabbit anti-β-galactosidase antibodies, the two antibodies were serially applied to immunohistochemical reaction.

Generation of Fkhl18-lacZ Transgenic (Tg) Mice

Cosmid genomic clones containing mouse *Fkhl18* gene were obtained from a cosmid library constructed with SuperCos-1 cosmid vector (Stratagene, La Jolla, CA) carrying hsp68-lacZ cassette (Fig. 2A). This cosmid vector was constructed to examine the enhancer activity of inserted DNAs (Zubair et al., 2006). Genomic DNAs containing 3′ regions of *Fkhl18* prepared from cosmid clone were ligated with hsp68-lacZ (Zubair et al., 2006) cassette to construct plasmids for Tg mice (Fig. 2A). The cosmid and plasmid DNAs were digested with *Not*I and *Not*I/*Sal*I, respectively, and the linear DNA fragments were used for microinjection. Tg mice were generated as described previously (Nagy et al., 2003). The DNAs of the founder animals were subjected to PCR with primers for lacZ (5′-GCC GAA ATC CCG AAT CTC TAT C-3′ and 5′-GAT TCA TTC CCC AGC GAC CAG-3′). LacZ activities of the fetuses were examined as described previously (Nagy et al., 2003).

Generation of Fkhl18 KO Mice

Fkhl18 gene is comprised by a single exon. Bacteriophage clones containing *Fkhl18* gene were obtained from 129/SvEv genomic library (Stratagene). To disrupt *Fkhl18* gene, a *Nco*I/*Kpn*I fragment of *Fkhl18* gene was substituted by IRES-lacZ-pMC1-Neo cassette (Katoh-Fukui et al., 1998; Kitamura et al., 2002). The 5′ region from the *Not*I site (0.9 kb) and 3′ region from the *Kpn*I site (6.7 kb) were used for homologous recombination (Fig. 3). The targeting linearized vector was subjected to electroporation into E14TG2a (129Ola) ES cell line (Kitamura et al., 2002). The chimeric male mice produced with the homologous recombinant ES clones were crossed with C57BL/6Jjcl females (Japan Clea). *Fkhl18* deficient heterozygous male mice obtained were backcrossed onto C57BL/6Jjcl genetic background. Three to seven generations of the mice were used to obtain homozygous *Fkhl18* KO mice. Littermates were genotyped by PCR with the following primers; Fkh3-110FW (5′-CCT CCT GAC AAA CTT GGG ATG T-3′), Fkh3-109RV (5′- TTG TGG AGG AGA CTA AGC CAC CT-3′), and OIMR014 (5′-AGG TGA GAT GAC AGG AGA TC-3′) (Fig. 3).

All animal experiments were carried out in accordance with National Institute of Health Guide for the Care and Use of Laboratory Animals and approved by the Animal Care and Use Committee of National Institute for Basic Biology.

Electron Microscopy

Wild-type (WT) and *Fkhl18* KO testes were excised from fetuses and immersed in 3% glutaraldehyde in 10 mM HEPES (*N*-2-hydroxylpiperazine-*N*′-2-ethanesulfonic acid)–NaOH (pH 7.4) and 145 mM NaCl for at least 2 hr. After fixation with 1% osmium tetroxide for 1 hr, the tissues were dehydrated and embedded in epoxy resin. Ultrathin sections were prepared, stained with uranyl acetate and lead citrate, and thereafter subjected to electron microscopic observation. Electron micrographs were taken with a JEM 1200EX electron microscope (JOEL, Tokyo, Japan) as described previously (Katoh-Fukui et al., 2005).

Visualizing Fetal Vasculature System by Ink Injection

Ink was injected as described previously (Nagy et al., 2003). E14.5 fetuses were dissected from a pregnant female with an intact yolk sac and attached placenta. The fetuses were placed in PBS at 37°C under a dissecting scope, to be kept circulation active. The tip of a glass pipette was inserted into the umbilical vessel, and carbon ink (CE 100-6, Kuretake Co., Nara, Japan) was instilled into the vessel with minute puffs of breath. The diameter of the carbon particle is longer than 50 nm (average, 180 nm). After distribution of the ink in whole body, the fetus was fixed with 4% PFA. The gonads were harvested and examined under a light microscope. To analyze the testicular distribution of the injected ink, the fetuses were cryosectioned into 10-μm thick sections.

Reporter Gene Assay and Immunocytochemistry

Full-length *Fkhl18* coding region was subcloned into pcDNA3 expression vector (Invitrogen). p6 × DBE-luc reporter plasmid carrying six repeats of Fox binding sequence, and expression vectors for FoxO3 and FoxO4 (Furuyama et al., 2000) were kindly provided by Dr. T. Furuyama (Sonoda Women's University). Human and mouse Fas ligand (*FasL*) gene promoter regions were prepared by PCR with genomic DNAs of HEK293 and Y1 cells, respectively. PCR (94°C for 15 sec, 60°C for 30 sec, 68°C for 1 min 30 sec, 30 cycles) was performed using the following primers for human *FasL* promoter, KpnI-hFasL-1500 s (5′-ATG GTA CCC CAT GTA TTT CAT CTG GCA ACC ATA AC-3′) and hFasL-1-HindIII as (5′-GCA AGC TTG GCA GCT GGT GAG TCA GGC CAG CC-3′), and for mouse *FasL* promoter, KpnI-mFasL-1534 s (5′-ATG GTA CCG TGA TTG GTG GAC AGT AGG GTG TTG-3′) and mFasL-1-HindIII as (5′-GCA AGC TTG GCA CCC AGC CCC AGG AAA GGG TTT C-3′). Approximately 1.5 kb PCR products were subcloned into pGL3-basic (Promega, Madison, WI). Human osteosarcoma U2OS cells and primary cultures of bovine aortic smooth muscle cells (Aoyama et al., 2000) were grown in Dullbecco's modified Eagle's medium (DMEM; Sigma) supplemented with 10% fetal bovine serum and 1× penicillin–streptomycin–glutamine (Invitrogen) at 5% CO_2 and 37°C. Transfection was performed as described previously (Mukai et al., 2002). pCMV-SPORT-β-gal (Invitrogen) was used as an internal control to normalize transfection efficiency. The cells were harvested 48 hr after transfection, and the cell lysates were subjected to luciferase and β-galactosidase assays as described previously (Mukai et al., 2002). All transfection experiments were performed in triplicate. Values are presented as mean ± standard deviation (SD) of three independent experiments.

For immunocytochemistry, U2OS cells were seeded on coverslips and then subjected to transfection as described above. The cells were fixed 48 hr after transfection in 4% PFA, blocked with 1.5% skim milk, and then incubated with anti-myc (N-14, Santa Cruz Biotechnology, Santa Cruz, CA) and anti-HA (12CA5) antibodies. For fluorescent detection, Alexa Fluor 488 anti-rabbit antibody (Invitrogen) and Cy3 anti-mouse antibody (Invitrogen) were used, respectively. Nuclei were counterstained with DAPI (Sigma).

Electrophoretic Mobility Shift Assay (EMSA)

Double-stranded oligonucleotides containing 5′ protruding ends were labeled with ^{32}P-dCTP and Klenow polymerase. The nucleotide sequences for the probes were 5′-GATCAAGTAAACAACTATGT-3′/5′-CTAGACATAGTTGTTTACTT-3′ for WT probe and 5′-GATCAAGTAAGCAACTATGT-3′/5′-CTAGACATAGTTGCTTACTT-3′ for mutated probe (underlined nucleotide are mutated). Fkhl18-myc was prepared using a coupled TNT transcription and translated kit (Promega). EMSA was performed as described previously (Morohashi et al., 1992).

RESULTS

Expression of Fkhl18 in Periendothelial and Sertoli Cells of Fetal Testis

To examine the tissue specificity of *Fkhl18* expression during mouse fetal development, RT-PCR was performed with RNAs prepared from various tissues at E16.5 (Fig. 1A). Although the expression of *Fkhl18* was detected in many tissues examined, the expression in the testis was clearly higher than others including the ovary. Next, we determined the type of fetal testicular cells that expressed *Fkhl18* by in situ hybridization. The in situ signals were detected both inside and outside (interstitial region) of the testis cord (Fig. 1B-a). Immunohistochemical staining with anti-Ad4BP/SF-1 after the in situ analysis showed that Ad4BP/SF-1 immunoreactive nuclei are surrounded by in situ signals in the testicular cord (Fig. 1B-b, arrows), strongly suggesting that *Fkhl18* is expressed in Sertoli cells.

The interstitial region of the developing fetal testis is occupied by different cell types, such as fetal Leydig cells, peritubular cells, periendothelial cells (pericytes), endothelial cells, and uncharacterized fibroblast-like cells. Moreover, a large coelomic vessel is characteristic for the fetal testis. Vascular blood vessels are generally composed of endothelial cells and vascular smooth muscle cells, which encircle endothelial cells to act as a supporting structure of the vessel. However, at the early stage of blood vessel formation, vascular smooth muscle cells are still immature and thus referred as periendothelial cells. To identify the cells that express *Fkhl18*, we localized PECAM1-positive endothelial cells in sections next to those used for in situ hybridization for *Fkhl18*. As shown in Figure 1B, the PECAM1-positive endothelial cells of the coelomic vessel (Fig. 1B-c) and inner testicular vessel (Fig. 1B-e) seemed to be encircled by

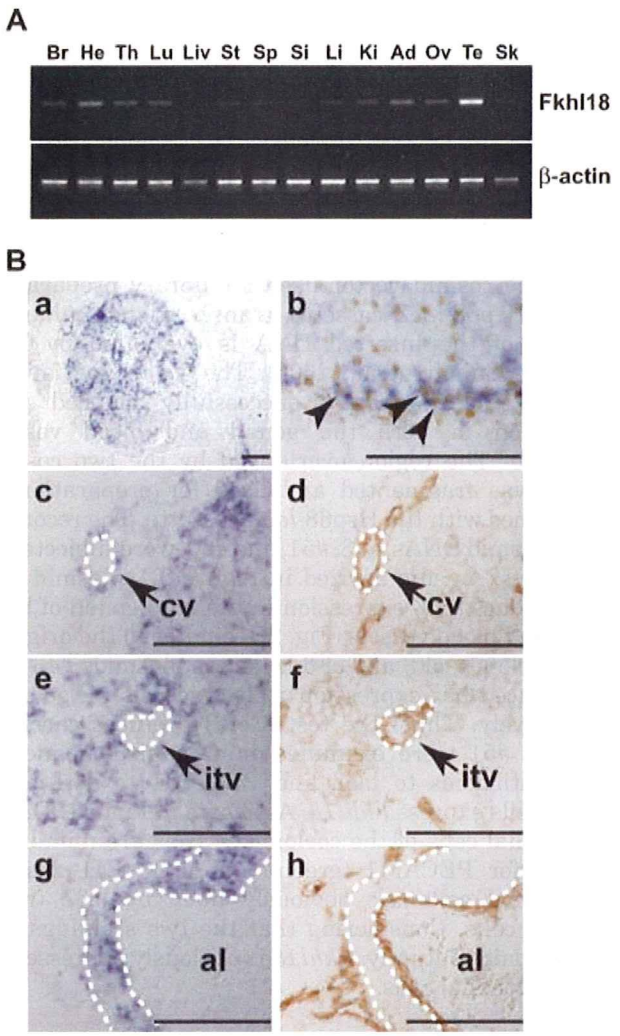

Fig. 1. Expression of Fkhl18 in the developing tissues of mouse fetuses. **A**: Analyses of *Fkhl18* gene expression by RT-PCR. Total RNAs prepared from E16.5 fetal tissues were subjected to RT-PCR with sets of primer for *Fkhl18* and β-actin. Br; brain, He; heart, Th; thymus, Lu; lung, Liv; liver, St; stomach, Sp; spleen, Si; small intestine, Li; large intestine, Ki; kidney, Ad; adrenal gland, Ov; ovary, Te; testis, Sk; skin. **B**: Expression of *Fkhl18* in E14.5 male gonad. In situ hybridization probed with *Fkhl18* was performed with E14.5 male gonad (a, b, c, e). The section used for in situ hybridization was further subjected to immunohistochemistry with antibody for Ad4BP/SF-1 (b). As indicated by arrowheads in (b), Sertoli cells in the testis cord are double positive for *Fkhl18* and Ad4BP/SF-1. Cells surrounding the coelomic vessel (cv; indicated by dotted line in c) and inner testis vessel (itv; indicated by dotted line in e) provided the in situ signals. *Fkhl18* in situ signal surrounding an aorta (g) is shown (g). al; aortic lumen. Sections next to (c), (e), and (g) were subjected to immunostaining with antibody to PECAM1 in (d), (f), and (h), respectively. Scale bars = 100 μm.

Fkhl18-expressing cells (Fig. 1B-d,f). Likewise, examination of the aorta showed a similar correlation of expressions between *Fkhl18* and PECAM1 (Fig. 1B-g,h). These expression profiles of *Fkhl18* and PECAM1 suggest that *Fkhl18* is expressed in periendothelial cells. To confirm this, we tried to perform double staining for *Fkhl18* in situ and PECAM1 immunohistochemistry. Unfortunately, however, immunohistochemistry with PECAM1 did not work after the

reaction of in situ hybridization. Moreover, we attempted to prepare antisera for *Fkhl18*, but could not obtain any antisera applicable for immunohistochemical study.

Instead, we generated transgenic (Tg) mice with *lacZ* reporter gene to recapitulate the endogenous expression of *Fkhl18*. Cosmid clones, cF6 and cF8 (Fig. 2A), carrying whole genomic regions of intron-less *Fkhl18* were obtained by screening of a mouse cosmid library. Since the cosmid vector used for library preparation carries Hsp68-*lacZ* cassette, transcriptional enhancer activity of the inserted DNA is evaluated by lacZ staining (Zubair et al., 2006). The Tg mouse fetuses harboring cF6 and cF8 successfully induced *lacZ* expression in both the gonad and blood vessels (Fig. 2B). The region overlapped by the two cosmid DNAs was fragmented and used for preparation of transgenes with the Hsp68-*lacZ* cassette. The recombinant plasmid DNAs, #43, #51, and #60, were subjected to Tg assays. As summarized in Figure 2B, plasmid #51 could induce *lacZ* expression in the fetal gonad of both sexes and blood vessels (Fig. 2C) similar to the original cosmid clones, cF8 and cF6, whereas plasmids #43 and #60 induced *lacZ* expression in blood vessels and gonads, respectively. Thus, the testes of Tg fetuses carrying plasmid #51 were examined immunohistochemically with antibodies to lacZ and PECAM1 to determine which cells express *Fkhl18*. As shown in Figure 2D, the endothelial cells of the coelomic vessels are immunoreactive for PECAM1 (green), and PECAM1-positive endothelial cells are obviously lined by lacZ (red)-positive cells. Considering that the two stainings are not overlaid mutually, *Fkhl18* is obviously expressed in periendothelial cells.

Abnormal Testicular Vasculature in Fkhl18 Deficient Mice

To investigate the function of *Fkhl18*, we generated a gene disrupted mouse. The *Nco*I/*Kpn*I fragment of the *Fkhl18* gene encoding from 29th to 329th amino acid residues was replaced by IRES-lacZ-pMC1neo cassette (Fig. 3A). *Fkhl18* disrupted allele was confirmed by Southern blotting (Fig. 3B,C) and PCR (Fig. 3D). The resultant heterozygous crosses yielded homozygous, heterozygous, and WT individuals at Mendelian ratios when examined at fetal life and adulthood (data not shown). Expectedly, *Fkhl18* mRNA was depleted from the *Fkhl18* KO testes (Fig. 3E). Although the reason was not clear, we could not detect any lacZ signals in the heterozygous and KO fetuses.

The homozygous *Fkhl18* KO male and female mice were healthy and fertile. Being consistent with unaffected fertility, Sertoli cells in the KO testes were apparently normal. However, we noticed accumulation of blood in the central part of the testes in *Fkhl18* KO mice (Fig. 4A). The incidence of this abnormal feature was 33% in homozygous KO but 0% in the WT, when examined in the testes of 14 WT, 26 heterozygous, and 12 homozygous KO (Fig. 4B). Interestingly, this phenotype was observed even in the heterozygous testes and the frequency seemed to correlate with the dosage of the gene.

To visualize the entire structure of the testicular vasculature system, we injected carbon ink into the umbilical vein of E14.5 fetuses. Although the whole view of branches of the vasculature system was indistinguishable between the WT and *Fkhl18* KO testes (Fig. 4C-a,b), the area around the vasculature looked

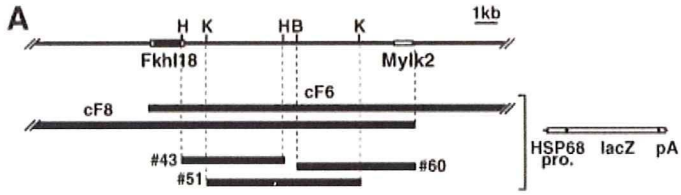

B

	TG	gonad	blood vessel
cF8	4	3	3
cF6	2	2	2
#43	3	0	3
#60	2	2	0
#51	5	4	4

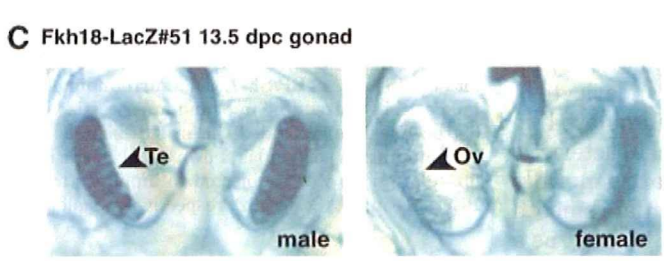

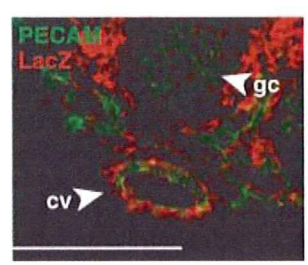

Fig. 2. Expression of Fkhl18 in the periendothelial cells of mouse fetal testis. **A**: DNA construction for Tg mouse assay. Cosmid clones, cF6 and cF8, were isolated from a library prepared with cosmid vector carrying hsp68-lacZ cassette. A region overlapped by these two cosmid clones was fragmented and ligated to hsp68-lacZ cassette to produce plasmid clones, #43, #51, and #60. H; *Hin*dIII, K; *Kpn*I, B; *BamH*I. **B**: Summary of Tg assays with the recombinant Tg constructs. The cosmid (cF6 and cF8) and plasmid (#43, #51, and #60) recombinant DNAs were used to generate Tg mice, and lacZ expression in the fetal gonad and blood vessel was examined at E13.5. Numbers represent those of Tg fetuses examined, and those displaying lacZ activity in the gonad and blood vessels. **C**: LacZ expression in Tg mice. Tg mice were produced with the #51 recombinant DNA. Representative expression patterns of *lacZ* are shown in male (left) and female (right) fetuses at E13.5. Te; testis, Ov; ovary. **D**: Expression of *LacZ* in periendothelial cells. The testis of the Tg fetus (#51) at E14.5 was subjected to immunohistochemical analyses with antibodies to PECAM1 (green) and lacZ (red). Note the signals for PECAM1 in endothelial cells of coelomic vessel (cv) and germ cells (gc). Note also signal for lacZ in periendothelial cells.

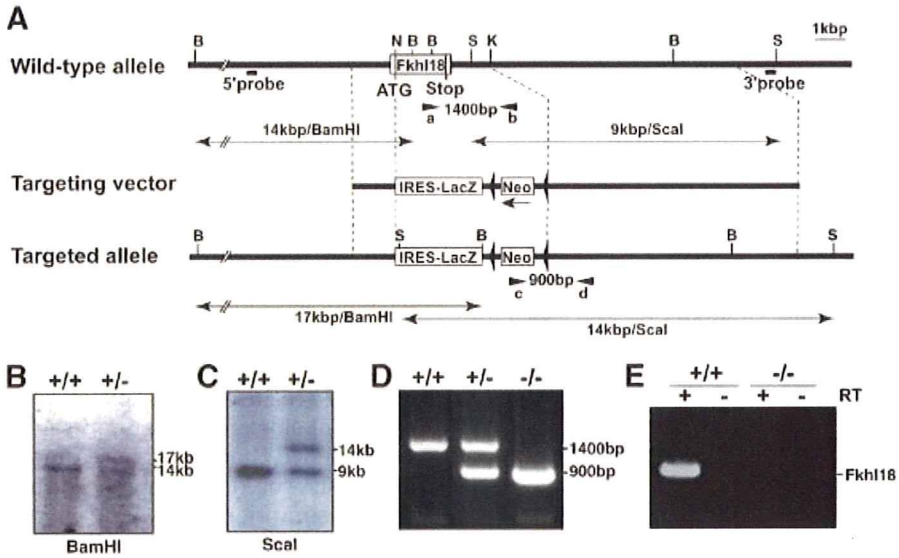

Fig. 3. Generation of *Fkhl18* KO mice. **A**: Generation of targeted allele of *Fkhl18*. Wild-type (WT) *Fkhl18* locus (top), targeting vector (middle), and targeted locus (bottom) are shown. *Fkhl18* gene consists of a single exon. Shaded and open boxes indicate coding and noncoding regions, respectively. The *Nco*I/*Kpn*I fragment of *Fkhl18* gene encoding 29th to 329th amino acid residues was replaced by IRES-lacZ-pMC1neo cassette in the targeting vector. Homologous recombination between the WT and targeting vector is expected to generate the targeted allele lacking the *Nco*I/*Kpn*I fragment. B; *Bam*HI, S; *Sca*I, N; *Nco*I. K; *Kpn*I. **B**: Southern blotting of *Bam*HI digested tail DNA from WT (+/+) and heterozygous (+/−) for *Fkhl18* KO. After the *Bam*HI digested DNAs were separated by agarose gel electrophoresis, the DNAs transferred to membrane were hybridized with the 5′ probe indicated in (A). The 5′ probe detected a 14-kb fragment in the WT mouse, and both 14-kb and 17-kb fragments in the heterozygous mouse. **C**: Southern blotting of *Sca*I digested tail DNA from WT (+/+) and heterozygous (+/−) for *Fkhl18* KO. The DNAs were hybridized with the 3′ probe is indicated in (A). The 3′ probes detected a 9 kb fragment in the WT mouse, and both 9 and 14 kb fragments in the heterozygous mouse. **D**: Genomic PCR to distinguish homozygous, heterozygous, and WT for *Fkhl18* KO. Genomic DNAs were extracted from tails of the fetuses and subjected to PCR analyses using primers a and b, and c and d. PCR product of 1.4 kb length is detected in the WT (+/+), both 1.4 and 0.9 kb are detected in the heterozygous (+/−), and 0.9 kb is detected in homozygous (−/−) fetuses. **E**: RT-PCR analyses of *Fkhl18* expression. Total RNAs were prepared from E14.5 fetal testes of the WT (+/+) and homozygous (−/−) KO, and were analyzed by RT-PCR.

dark and blurred in the *Fkhl18* KO testes. Thus, the gonads were sectioned, and we found leaking of the injected carbon ink from the testicular vessels (Fig. 4C-c,d) and coelomic vessel (Fig. 4C-e,f). The leakage of the carbon ink suggested a defect in the sealing structure of the vasculature in the *Fkhl18* KO mice. Further examination of the fine structure of the testicular vasculature by electron microscopy showed the presence of hole in the endothelial cells of the *Fkhl18* KO testes; the holes varied in size from 100 to 400 nm were devoid of any membrane and allowed extravasation of carbon ink (Fig. 4D). Usually, one gap was noticed in every 10 cross sections of capillaries. Obvious defect was not observed in the periendothelial cells. Any abnormality was never seen in the vasculature of WT.

Apoptosis of Periendothelial Cells in Fkhl18 KO Fetal Testis

The above structural defect suggested ectopic apoptosis of cells in the vasculature system of the *Fkhl18* KO testis. To test this, we examined the expression of caspase 3 in the WT and KO testes. As expected, caspase 3-positive cells (green in Fig. 5A) were found adjacent to vascular endothelial cells (red in Fig. 5A) in the KO testes. Considering the spatial correlation between caspase 3-positive cells and PECAM1-positive endothelial cells, we concluded that the apoptotic cells were periendothelial cells. To confirm this, we used *Fkhl18* KO mouse harboring #51 Tg construct (Fkhl18KO; Fkhl18-lacZ Tg). As shown in Figure 5B, caspase 3-positive signals overlapped with lacZ staining. The density of apoptotic cells in the KO testes was approximately threefold that in the WT (n = 4 fetuses each; Fig. 5C). These findings suggest that apoptosis of periendothelial cells in the absence of *Fkhl18* leads to defective testicular vascular system.

Possible Involvement of Fkhl18 in Regulation of Fas Ligand Gene Expression

Fox proteins share a winged helix DNA-binding domain and are known to act as transcription factors. To investigate whether Fkhl18 have a transcriptional activity, we performed reporter gene assays using p6 × DBE-luc containing six repeats of Fox consensus sequence. As described previously (Furuyama et al., 2000), both FoxO3a and FoxO4 activated the transcription of p6 × DBE-luc, whereas *Fkhl18* did not show any activity by itself (Fig. 6A). Therefore, we examined whether *Fkhl18* acts as a suppressor against FoxO3a and FoxO4. When Fkhl18 was co-expressed with FoxO3a or FoxO4, the activities driven by FoxO3a and FoxO4 were suppressed in a dose-dependent manner (Fig. 6A).

Next, we examined the DNA binding activity of Fkhl18 by EMSA (Fig. 6B). In vitro synthesized myc-tagged Fkhl18 bound to Fox consensus sequence (WT)

but not to mutated sequence (mut), and this binding signal disappeared in a dose-dependent manner following the addition of nonlabeled WT oligonucleotides. The results of the in vitro EMSA study suggest that the transcriptional suppression by Fkhl18 is due to competitive binding between Fkhl18 and FoxOs, although it was unknown whether Fkhl18 is localized in the nucleus or not. To check this, we examined intracellular distribution of myc-tagged Fkhl18 (Fkhl18-myc) in cultured cells. As shown in Figure 6C, FoxO3 and FoxO4 were localized exclusively in the nucleus, while Fkhl18 was localized predominantly in the nucleus. Together with the results of the reporter gene assays, it is likely that Fkhl18 suppresses the activities of other Fox proteins possibly through competitively occupying the target site on gene promoters.

As described above, our study showed that disruption of *Fkhl18* resulted in ectopic apoptosis of periendothelial cells. Considering the suppressive function of Fkhl18, we assumed that genes necessary for the occurrence of apoptosis would be suppressed in WT. Consistent with this assumption, it was reported that *FasL* gene expression is activated by Fox proteins (Brunet et al., 1999). Therefore, we investigated whether Fkhl18 suppresses human and mouse *FasL* promoter activities. As we expected, Fkhl18 suppressed, dose-dependently, human and mouse *FasL* promoter in bovine vascular smooth muscle cells (Fig. 6D). Considered together, these results suggest that Fkhl18 potentially suppresses proapoptotic signals by associating the Fox consensus element in *FasL* promoter.

DISCUSSION

Development of the vascular system of animals starts at fetal age. Primitive vasculature consisting of small capillaries develops from blood vessel precursor cells, and the primitive vessels expand progressively, producing branches to form the vascular tree. At the early stage of blood vessel formation (angiogenesis and arteriogenesis), periendothelial cells as well as endothelial cells are required for generation of a functional vascular system (Carmeliet, 2003, 2005). The requirement of endothelial and periendothelial cells is strongly suggestive of a functional correlation between the two cell types during blood vessel development. In the present study, we demonstrated the expression of *Fkhl18* in periendothelial cells encircling the endothelial cells in the

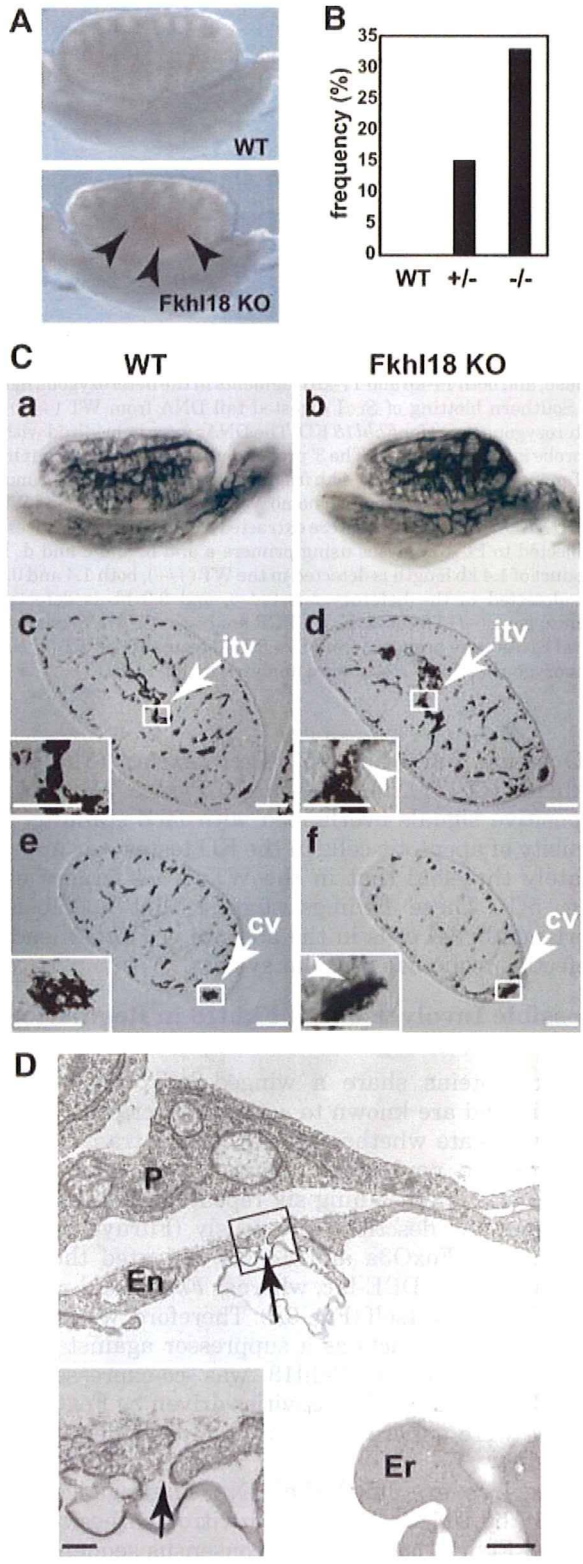

Fig. 4. Testicular vasculature abnormalities in *Fkhl18* KO mice. **A**: Appearance of dissected fetal testes of WT and *Fkhl18* KO. Note the accumulation of blood cells in the central part of the *Fkhl18* KO testis (arrowheads). **B**: Frequency of blood accumulation examined in 14 WT, 26 heterozygous (+/−) and 12 homozygous (−/−) testes. Frequency (%) of testes showing blood accumulation relative to total number of testes examined are shown. **C**: Visualization of the vasculature structure using carbon ink. Carbon ink was injected into the testes through the umbilical vein. The whole views of the WT (a) and *Fkhl18* KO testes (b) are shown. The WT (c, e) and *Fkhl18* KO (d, f) testes were sectioned. Areas containing inner testicular vessels (itv; c, d) and coelomic vessels (cv; e, f) are enlarged in insets. As indicated by arrowheads in insets of (d) and (f), leakage of the injected ink was noted around the vessels of *Fkh18* KO testes. Scale bars = 100 μm, scale bars in insets = 50 μm. **D**: Electron microscopic view of a representative *Fkhl18* KO testis. The area enclosed by the rectangle is enlarged as the inset. Arrows indicate a gap in endothelial cells in KO testis. En; endothelial cell, P; periendothelial cell, Er; erythrocyte. Scale bars = 500 μm, scale bars in insets = 100 μm.

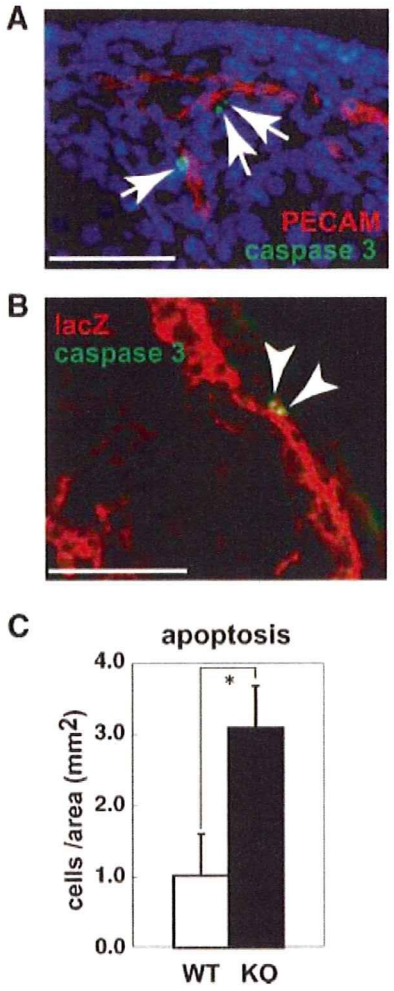

Fig. 5. Marked apoptosis of periendothelial cells in *Fkhl18* KO testis. **A**: Expression of caspase 3 in the *Fkhl18* KO fetal testis. *Fkhl18* KO E14.5 testis was immunostained with caspase 3 antibody (green) and PECAM (red). As indicated by arrows, caspase 3-positive cells are localized adjacent to PECAM-positive endothelial cells (red). Nuclei were counterstained with DAPI (blue). Scale bars = 50 μm. **B**: Expression of caspase 3 in periendothelial cells of the *Fkhl18* KO fetal testis. Double immunostaining for lacZ and caspase 3 was performed in E14.5 testes of Fkhl18KO; Fkhl18-lacZ Tg mice. As indicated by arrowheads, caspase 3-positive cells (green) overlapped with Fkhl18-positive cells (red). Scale bars = 50 μm. **C**: Apoptosis of vascular periendothelial cells. Caspase 3-positive cells adjacent to endothelial cells were counted in WT and *Fkhl18* KO fetal testes. Data are mean ± SD numbers of caspase 3-positive cells per unit area (mm^2). $^*P < 0.02$.

developing fetal testis. *Fkhl18*-deficient mice displayed the following testicular abnormalities during fetal life; (1) accumulation of blood cells in the central part of the fetal testis, (2) presence of gaps, measuring 100–400 nm in diameter, in endothelial cells, allowing leakage of injected carbon ink from the testicular vessels, and (3) aberrant apoptosis of periendothelial cells. These features strongly suggest the importance of *Fkhl18* expression in the periendothelial cells for development of the testicular vascular system through direct and indirect regulation of the functions of periendothelial and endothelial cells, respectively.

This indirect function of *Fkhl18* indicates a functional interaction between endothelial and periendothelial cells. The importance of interactions between the two cell types for vascular maturation has been examined by gene knockout studies. For example, angiopoietin-1 is expressed in periendothelial cells, while its receptor *TIE-2* is expressed in endothelial cells. In the absence of periendothelial angiopoietin-1, endothelial cells do not properly recruit and associate with periendothelial supporting cells (Suri et al., 1996). This ligand/receptor interaction represents a signaling pathway from periendothelial to endothelial cells. As a reciprocal signaling pathway, functional correlation between platelet-derived growth factor (PDGF)-BB expressed in endothelial cells and PDGF receptor β (PDGFRβ) in periendothelial cells was demonstrated (Hellstrom et al., 1999). Recruitment of periendothelial cells expressing *PDGFRβ* was affected when *PDGF-BB* gene was disrupted. Unlike the KO mice described above, recruitment of periendothelial cells did not seem to be affected in the fetal testes of *Fkhl18* KO mice. Interestingly, however, marked apoptosis of periendothelial cells was observed; with resultant focal and transient loss of periendothelial cells. Since *Fkhl18* is not expressed in endothelial cells, the structural defect induced in endothelial cells possibly resulted from weakened interaction with the affected or decreased periendothelial cells.

Male-specific patterning of the vasculature in the developing testis is induced by *Sry* (Buehr et al., 1993; Martineau et al., 1997; Capel et al., 1999; Tilmann and Capel, 1999; Brennan et al., 2002, 2003). Following the expression of *Sry*, endothelial cells are recruited vigorously to the testis from mesonephros to develop the male specific coelomic vessel. Thereafter, the vessel branches from the coelomic vessel and extends progressively between testicular cords. Although blood vessels are also formed in the ovary, such active event of blood vessel formation never occurs in the ovary at the fetal stage. In this study, we noticed blood cell accumulation in the central part of the fetal testis in most *Fkhl18* KO fetuses. However, such defect was never seen in the female KO ovary (data not shown). This sexually dimorphic defect seems to correlate with the differential development of blood vessels in the two sexes. Moreover, the expression of *Fkhl18* in the testis is significantly higher than in the ovary. Taken together, higher amount of *Fkhl18* would be required for the active organization of the vasculature system.

Reporter gene assays revealed that Fkhl18 suppresses transcription mediated by *FoxO3a* and *FoxO4*. Since Fkhl18 can bind to consensus DNA binding sequence for *Fox*, it potentially represses transcription by competing for binding sites with other Fox proteins. Considering the suppressive function of Fkhl18, it is interesting to note that FoxOs mediate proapoptotic gene expression. For example, overexpression of FoxOs resulted in apoptosis through direct induction of tumor-necrosis factor-related apoptosis-inducing ligand (TRAIL) in prostate cancer (Modur et al., 2002). In neurons deprived of nerve growth factor (NGF), FoxO3a

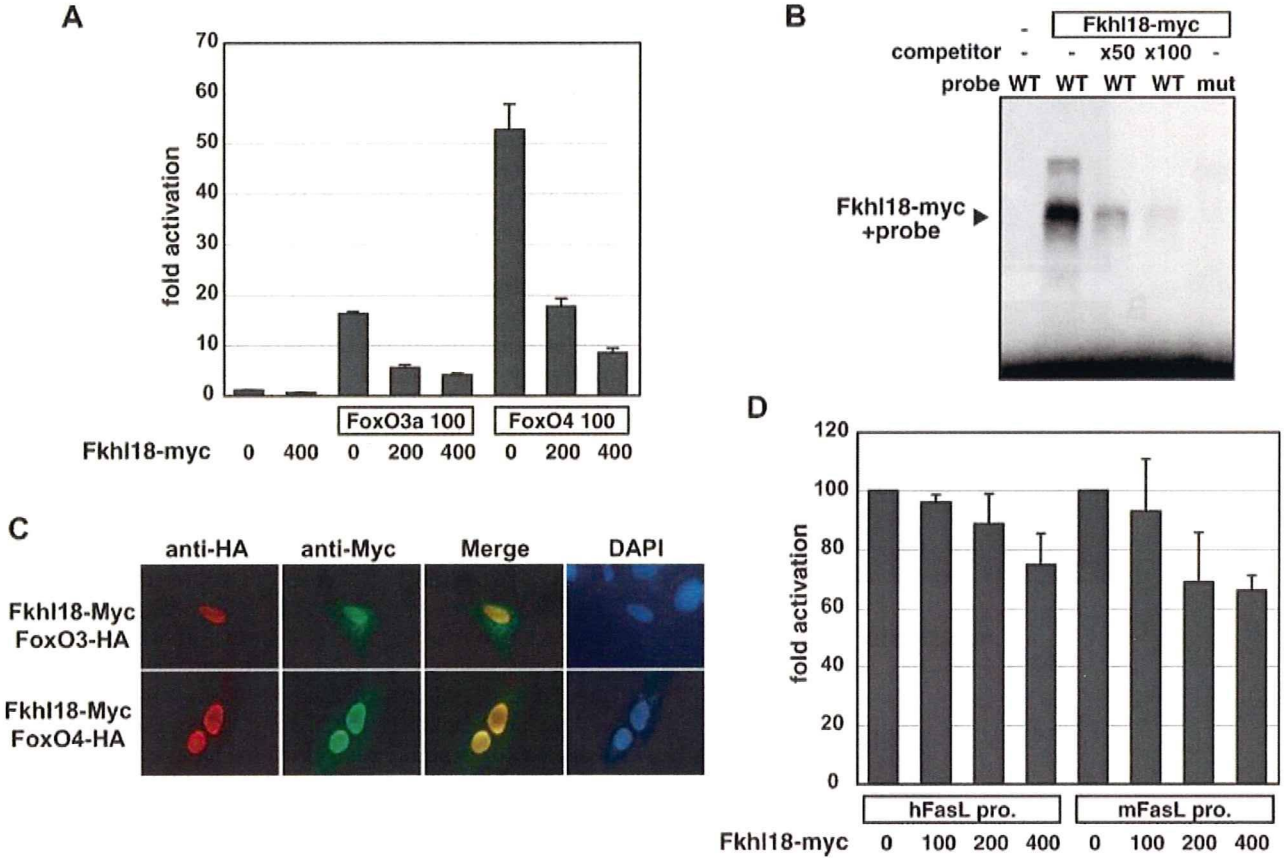

Fig. 6. Possible transcriptional suppression of Fas ligand gene by Fkhl18. **A**: Transcriptional suppression by Fkhl18. Expression vectors for Fkhl18 (400 ng) or FoxO3a (100 ng), FoxO4 (100 ng) were transfected into U2OS cells with p6 × DBE-luc reporter gene containing six repeats of consensus binding sequence for forkhead proteins (200 ng), and β-galactosidase (25 ng). For effects of Fkhl18 on FoxOs' activity, increasing amounts of Fkhl18 (200, 400 ng) were transfected with FoxO3a (100 ng) or FoxO4 (100 ng). Results are mean ± SD of triplicate transfections. Data represent the ratio of luciferase activity normalized by β-galactosidase activity to basal reporter activity. **B**: EMSAs performed with WT and mutated Fox consensus sequences. In vitro synthesized Fkhl18-myc was incubated with WT and mutated oligonucleotides (mut). Fifty or 100-fold excess amount of unlabeled oligonucleotide (WT) was used as a competitor. Arrowhead indicates retarded signal. **C**: Intracellular localization of Fkhl18. Fkhl18-myc (green), FoxO3-HA (HA-tagged FoxO3), and FoxO4-HA (HA-tagged FoxO4) were transfected into U2OS cells and their intracellular distribution was examined. Cells were counterstained with DAPI (blue). **D**: Suppressive effect of Fkhl18 on FasL promoter. Increasing amount of Fkhl18 expression vector (100, 200, 400 ng) were transfected into bovine vascular smooth muscle cells with human or mouse FasLpro-luc reporter gene (200 ng), and β-galactosidase (20 ng). Results are mean ± SD of three independent experiments. Data represent the ratio of luciferase activity normalized by β-galactosidase activity to basal reporter activity.

directly activated *bim* (Bcl-2 interacting mediator of cell death) promoter via conserved Fox binding sites (Gilley et al., 2003). Moreover, *Akt* activated by survival factors phosphorylated *FoxO3a* and thereby prevented the association of *FoxO3a* to *FasL* promoter (Brunet et al., 1999). Based on the results published so far, we hypothesized that the marked apoptosis of periendothelial cells in *Fkhl18* KO testes is caused by defective proapoptotic gene transcription, which is normally attenuated by Fkhl18. As expected, Fkhl18 suppressed transcription from *FasL* gene promoter in cultured smooth muscle cells prepared form bovine blood vessels, although such suppression seemed inefficient. We assumed that the inefficient suppression was due to cellular condition since normally *FasL* gene expression should be activated by apoptotic signal. Therefore, we carried out the reporter gene assays using cells treated with okadaic acid, which is known to activate the apoptotic process (Rossini et al., 1997; Goto et al., 2002; Fujita et al., 2004). Unfortunately, however, the reporter gene was probably abnormally transcribed, most likely because of the toxicity of okadaic acid (Rossini et al., 1997). Therefore, although the reason for the ineffective suppression by Fkhl18 remains to be clarified, it is possible that Fkhl18 modulates transcription driven by other Fox transcription factors in periendothelial cells.

In the present study, we focused on the function of *Fkhl18* during blood vessel formation of the fetal testis; blood vessel development in the ovary remains to be investigated. Likewise, we have not examined whether the blood vessels in tissues other than the gonads are affected by *Fkhl18*. Considering that *Fkhl18* is expressed in periendothelial cells of other tissues, the defects seen in the fetal testis could be also seen in other tissues. However, obvious accumulation of blood cells was not observed in any tissues other than the testis, strongly arguing against a major defect of blood vessel

development in these tissues. Together with the highest expression of *Fkhl18* in the developing testis, it is conceivable that *Fkhl18* plays a unique role in the development of the testicular vasculature system.

ACKNOWLEDGMENTS

We thank Dr. K. Mihara and Dr. M. Sakaguchi (Kyushu University) for providing antiserum to lacZ. This work was supported in part by Grants-in-Aid for Scientific Research (S) and Grants-in-Aid for Scientific Research on Priority Areas from the Ministry of Education, Culture, Sports Science, and Technology of Japan, and Japan Science and Technology Corporation.

REFERENCES

Accili D, Arden KC. 2004. FoxOs at the crossroads of cellular metabolism, differentiation, and transformation. Cell 117:421–426.

Ang SL, Rossant J. 1994. HNF-3 beta is essential for node and notochord formation in mouse development. Cell 78:561–574.

Aoyama T, Chen M, Fujiwara H, Masaki T, Sawamura T. 2000. LOX-1 mediates lysophosphatidylcholine-induced oxidized LDL uptake in smooth muscle cells. FEBS Lett 467:217–220.

Brennan J, Capel B. 2004. One tissue, two fates: Molecular genetic events that underlie testis versus ovary development. Nat Rev Genet 5:509–521.

Brennan J, Karl J, Capel B. 2002. Divergent vascular mechanisms downstream of Sry establish the arterial system in the XY gonad. Dev Biol 244:418–428.

Brennan J, Tilmann C, Capel B. 2003. Pdgfr-alpha mediates testis cord organization and fetal Leydig cell development in the XY gonad. Genes Dev 17:800–810.

Brice G, Mansour S, Bell R, Collin JR, Child AH, Brady AF, Sarfarazi M, Burnand KG, Jeffery S, Mortimer P, Murday VA. 2002. Analysis of the phenotypic abnormalities in lymphoedema-distichiasis syndrome in 74 patients with FOXC2 mutations or linkage to 16q24. J Med Genet 39:478–483.

Brunet A, Bonni A, Zigmond MJ, Lin MZ, Juo P, Hu LS, Anderson MJ, Arden KC, Blenis J, Greenberg ME. 1999. Akt promotes cell survival by phosphorylating and inhibiting a Forkhead transcription factor. Cell 96:857–868.

Buehr M, Gu S, McLaren A. 1993. Mesonephric contribution to testis differentiation in the fetal mouse. Development 117:273–281.

Capel B, Albrecht KH, Washburn LL, Eicher EM. 1999. Migration of mesonephric cells into the mammalian gonad depends on Sry. Mech Dev 84:127–131.

Carmeliet P. 2003. Angiogenesis in health and disease. Nat Med 9:653–660.

Carmeliet P. 2005. Angiogenesis in life, disease and medicine. Nature 438:932–936.

Castanet M, Park SM, Smith A, Bost M, Leger J, Lyonnet S, Pelet A, Czernichow P, Chatterjee K, Polak M. 2002. A novel loss-of-function mutation in TTF-2 is associated with congenital hypothyroidism, thyroid agenesis and cleft palate. Hum Mol Genet 11:2051–2059.

Chatila TA, Blaeser F, Ho N, Lederman HM, Voulgaropoulos C, Helms C, Bowcock AM. 2000. JM2, encoding a fork head-related protein, is mutated in X-linked autoimmunity-allergic disregulation syndrome. J Clin Invest 106:R75–R81.

Chen X, Rubock MJ, Whitman M. 1996. A transcriptional partner for MAD proteins in TGF-beta signalling. Nature 383:691–696.

Chen X, Weisberg E, Fridmacher V, Watanabe M, Naco G, Whitman M. 1997. Smad4 and FAST-1 in the assembly of activin-responsive factor. Nature 389:85–89.

Crisponi L, Deiana M, Loi A, Chiappe F, Uda M, Amati P, Bisceglia L, Zelante L, Nagaraja R, Porcu S, Ristaldi MS, Marzella R, Rocchi M, Nicolino M, Lienhardt-Roussie A, Nivelon A, Verloes A, Schlessinger D, Gasparini P, Bonneau D, Cao A, Pilia G. 2001. The putative forkhead transcription factor FOXL2 is mutated in blepharophimosis/ptosis/epicanthus inversus syndrome. Nat Genet 27:159–166.

Erickson RP, Dagenais SL, Caulder MS, Downs CA, Herman G, Jones MC, Kerstjens-Frederikse WS, Lidral AC, McDonald M, Nelson CC, Witte M, Glover TW. 2001. Clinical heterogeneity in lymphoedema-distichiasis with FOXC2 truncating mutations. J Med Genet 38:761–766.

Frank J, Pignata C, Panteleyev AA, Prowse DM, Baden H, Weiner L, Gaetaniello L, Ahmad W, Pozzi N, Cserhalmi-Friedman PB, Aita VM, Uyttendaele H, Gordon D, Ott J, Brissette JL, Christiano AM. 1999. Exposing the human nude phenotype. Nature 398:473–474.

Fujita M, Goto K, Yoshida K, Okamura H, Morimoto H, Kito S, Fukuda J, Haneji T. 2004. Okadaic acid stimulates expression of Fas receptor and Fas ligand by activation of nuclear factor kappa-B in human oral squamous carcinoma cells. Oral Oncol 40:199–206.

Furuyama T, Nakazawa T, Nakano I, Mori N. 2000. Identification of the differential distribution patterns of mRNAs and consensus binding sequences for mouse DAF-16 homologues. Biochem J 349:629–634.

Galili N, Davis RJ, Fredericks WJ, Mukhopadhyay S, Rauscher FJ III, Emanuel BS, Rovera G, Barr FG. 1993. Fusion of a fork head domain gene to PAX3 in the solid tumour alveolar rhabdomyosarcoma. Nat Genet 5:230–235.

Gilley J, Coffer PJ, Ham J. 2003. FOXO transcription factors directly activate bim gene expression and promote apoptosis in sympathetic neurons. J Cell Biol 162:613–622.

Goto K, Fukuda J, Haneji T. 2002. Okadaic acid stimulates apoptosis through expression of Fas receptor and Fas ligand in human oral squamous carcinoma cells. Oral Oncol 38:16–22.

Harris SE, Chand AL, Winship IM, Gersak K, Aittomaki K, Shelling AN. 2002. Identification of novel mutations in FOXL2 associated with premature ovarian failure. Mol Hum Reprod 8:729–733.

Hellstrom M, Kalen M, Lindahl P, Abramsson A, Betsholtz C. 1999. Role of PDGF-B and PDGFR-beta in recruitment of vascular smooth muscle cells and pericytes during embryonic blood vessel formation in the mouse. Development 126:3047–3055.

Hillion J, Le Coniat M, Jonveaux P, Berger R, Bernard OA. 1997. AF6q21, a novel partner of the MLL gene in t(6;11)(q21;q23), defines a forkhead transcriptional factor subfamily. Blood 90:3714–3719.

Hulander M, Wurst W, Carlsson P, Enerback S. 1998. The winged helix transcription factor Fkh10 is required for normal development of the inner ear. Nat Genet 20:374–376.

Hulander M, Kiernan AE, Blomqvist SR, Carlsson P, Samuelsson EJ, Johansson BR, Steel KP, Enerback S. 2003. Lack of pendrin expression leads to deafness and expansion of the endolymphatic compartment in inner ears of Foxi1 null mutant mice. Development 130:2013–2025.

Kaestner KH, Lee KH, Schlondorff J, Hiemisch H, Monaghan AP, Schutz G. 1993. Six members of the mouse forkhead gene family are developmentally regulated. Proc Natl Acad Sci USA 90:7628–7631.

Katoh-Fukui Y, Tsuchiya R, Shiroishi T, Nakahara Y, Hashimoto N, Noguchi K, Higashinakagawa T. 1998. Male-to-female sex reversal in M33 mutant mice. Nature 393:688–692.

Katoh-Fukui Y, Owaki A, Toyama Y, Kusaka M, Shinohara Y, Maekawa M, Toshimori K, Morohashi K. 2005. Mouse Polycomb M33 is required for splenic vascular and adrenal gland formation through regulating Ad4BP/SF1 expression. Blood 106:1612–1620.

Kitamura K, Yanazawa M, Sugiyama N, Miura H, Iizuka-Kogo A, Kusaka M, Omichi K, Suzuki R, Kato-Fukui Y, Kamiirisa K, Matsuo M, Kamijo S, Kasahara M, Yoshioka H, Ogata T, Fukuda T, Kondo I, Kato M, Dobyns WB, Yokoyama M, Morohashi K. 2002. Mutation of ARX causes abnormal development of forebrain and testes in mice and X-linked lissencephaly with abnormal genitalia in humans. Nat Genet 32:359–369.

Koopman P, Munsterberg A, Capel B, Vivian N, Lovell-Badge R. 1990. Expression of a candidate sex-determining gene during mouse testis differentiation. Nature 348:450–452.

Labosky PA, Winnier GE, Jetton TL, Hargett L, Ryan AK, Rosenfeld MG, Parlow AF, Hogan BL. 1997. The winged helix gene, Mf3, is required for normal development of the diencephalon and midbrain, postnatal growth and the milk-ejection reflex. Development 124: 1263–1274.

Lai CS, Fisher SE, Hurst JA, Vargha-Khadem F, Monaco AP. 2001. A forkhead-domain gene is mutated in a severe speech and language disorder. Nature 413:519–523.

Lin L, Miller CT, Contreras JI, Prescott MS, Dagenais SL, Wu R, Yee J, Orringer MB, Misek DE, Hanash SM, Glover TW, Beer DG. 2002. The hepatocyte nuclear factor 3 alpha gene, HNF3alpha (FOXA1), on chromosome band 14q13 is amplified and overexpressed in esophageal and lung adenocarcinomas. Cancer Res 62:5273–5279.

Martineau J, Nordqvist K, Tilmann C, Lovell-Badge R, Capel B. 1997. Male-specific cell migration into the developing gonad. Curr Biol 7:958–968.

Mears AJ, Jordan T, Mirzayans F, Dubois S, Kume T, Parlee M, Ritch R, Koop B, Kuo WL, Collins C, Marshall J, Gould DB, Pearce W, Carlsson P, Enerback S, Morissette J, Bhattacharya S, Hogan B, Raymond V, Walter MA. 1998. Mutations of the forkhead/winged-helix gene, FKHL7, in patients with Axenfeld-Rieger anomaly. Am J Hum Genet 63:1316–1328.

Modur V, Nagarajan R, Evers BM, Milbrandt J. 2002. FOXO proteins regulate tumor necrosis factor-related apoptosis inducing ligand expression. Implications for PTEN mutation in prostate cancer. J Biol Chem 277:47928–47937.

Morohashi K, Honda S, Inomata Y, Handa H, Omura T. 1992. A common trans-acting factor, Ad4-binding protein, to the promoters of steroidogenic P-450s. J Biol Chem 267:17913–17919.

Morohashi K, Iida H, Nomura M, Hatano O, Honda S, Tsukiyama T, Niwa O, Hara T, Takakusu A, Shibata Y., et al. 1994. Functional difference between Ad4BP and ELP, and their distributions in steroidogenic tissues. Mol Endocrinol 8:643–653.

Mukai T, Kusaka M, Kawabe K, Goto K, Nawata H, Fujieda K, Morohashi K. 2002. Sexually dimorphic expression of Dax-1 in the adrenal cortex. Genes Cells 7:717–729.

Nagy A, Gertsenstein M, Vintersten K, Behringer R. 2003. Manipulating the mouse embryo: A laboratory manual, 3rd edition. New York: Cold Spring Harbor Laboratory Press.

Nakae J, Biggs WH III, Kitamura T, Cavenee WK, Wright CV, Arden KC, Accili D. 2002. Regulation of insulin action and pancreatic beta-cell function by mutated alleles of the gene encoding forkhead transcription factor Foxo1. Nat Genet 32:245–253.

Ogg S, Paradis S, Gottlieb S, Patterson GI, Lee L, Tissenbaum HA, Ruvkun G. 1997. The Fork head transcription factor DAF-16 transduces insulin-like metabolic and longevity signals in C. elegans. Nature 389:994–999.

Parry P, Wei Y, Evans G. 1994. Cloning and characterization of the t(X;11) breakpoint from a leukemic cell line identify a new member of the forkhead gene family. Genes Chromosomes Cancer 11:79–84.

Pierrou S, Hellqvist M, Samuelsson L, Enerback S, Carlsson P. 1994. Cloning and characterization of seven human forkhead proteins: Binding site specificity and DNA bending. EMBO J 13:5002–5012.

Renfree MB, Harry JL, Shaw G. 1995. The marsupial male: A role model for sexual development. Philos Trans R Soc Lond B Biol Sci 350:243–251.

Rossini GP, Pinna C, Viviani R. 1997. Inhibitors of phosphoprotein phosphatases 1 and 2A cause activation of a 53 kDa protein kinase accompanying the apoptotic response of breast cancer cells. FEBS Lett 410:347–350.

Semina EV, Brownell I, Mintz-Hittner HA, Murray JC, Jamrich M. 2001. Mutations in the human forkhead transcription factor FOXE3 associated with anterior segment ocular dysgenesis and cataracts. Hum Mol Genet 10:231–236.

Sinclair AH, Berta P, Palmer MS, Hawkins JR, Griffiths BL, Smith MJ, Foster JW, Frischauf AM, Lovell-Badge R, Goodfellow PN. 1990. A gene from the human sex-determining region encodes a protein with homology to a conserved DNA-binding motif. Nature 346:240–244.

Sorensen PH, Lynch JC, Qualman SJ, Tirabosco R, Lim JF, Maurer HM, Bridge JA, Crist WM, Triche TJ, Barr FG. 2002. PAX3-FKHR and PAX7-FKHR gene fusions are prognostic indicators in alveolar rhabdomyosarcoma: A report from the children's oncology group. J Clin Oncol 20:2672–2679.

Suri C, Jones PF, Patan S, Bartunkova S, Maisonpierre PC, Davis S, Sato TN, Yancopoulos GD. 1996. Requisite role of angiopoietin-1, a ligand for the TIE2 receptor, during embryonic angiogenesis. Cell 87:1171–1180.

Teh MT, Wong ST, Neill GW, Ghali LR, Philpott MP, Quinn AG. 2002. FOXM1 is a downstream target of Gli1 in basal cell carcinomas. Cancer Res 62:4773–4780.

Tilmann C, Capel B. 1999. Mesonephric cell migration induces testis cord formation and Sertoli cell differentiation in the mammalian gonad. Development 126:2883–2890.

Winnier GE, Hargett L, Hogan BL. 1997. The winged helix transcription factor MFH1 is required for proliferation and patterning of paraxial mesoderm in the mouse embryo. Genes Dev 11:926–940.

Zubair M, Ishihara S, Oka S, Okumura K, Morohashi K. 2006. Two-step regulation of Ad4BP/SF-1 gene transcription during fetal adrenal development: Initiation by a Hox-Pbx1-Prep1 complex and maintenance via autoregulation by Ad4BP/SF-1. Mol Cell Biol 26:4111–4121.

Volume 56(8): 773–784, 2008
Journal of Histochemistry & Cytochemistry
http://www.jhc.org

ARTICLE

Expression and Localization of Lectin-like Oxidized Low-density Lipoprotein Receptor-1 (LOX-1) in Murine and Human Placentas

Hiroo Satoh, Emi Kiyota, Yasuhiro Terasaki, Tatsuya Sawamura, Katsumasa Takagi, Hiroshi Mizuta, and Motohiro Takeya

Department of Cell Pathology (HS,EK,YT,MT) and Department of Orthopaedic and Neuro-Musculoskeletal Surgery (HS,KT, HM), Graduate School of Medical and Pharmaceutical Sciences, Kumamoto University, Kumamoto, Japan, and Department of Vascular Physiology, National Cardiovascular Center Research Institute, Osaka, Japan (TS)

SUMMARY Lectin-like oxidized low-density lipoprotein receptor-1 (LOX-1) is one of the scavenger receptors that recognizes oxidized low-density lipoprotein as a major ligand. The placenta is a major source of prooxidant during pregnancy, and the level of placental oxidative stress increases rapidly at the end of the first trimester and tapers off later in gestation. In our study, we evaluated placental expression of LOX-1 during different gestational stages in mice and humans. We used immunohistochemistry and ISH to identify LOX-1–expressing cells in murine and human placentas. In both species, higher expression of LOX-1 mRNA during early to midgestational stages compared with late gestation—corresponding to the increased oxidative stress in early pregnancy—was shown by real-time RT-PCR. In murine placenta, we showed that LOX-1–expressing cells were fibroblast-like stromal cells in metrial glands and decidua basalis and that they were glycogen trophoblast cells in the junctional and labyrinth zones. In the human, LOX-1 expression was detected in villous cytotrophoblasts in both first trimester and term placentas. These localization patterns of LOX-1 in murine and human placentas suggest the possible involvement of LOX-1 in high oxidative stress conditions of pregnancy. **(J Histochem Cytochem 56:773–784, 2008)**

KEY WORDS
LOX-1
placenta
glycogen trophoblast cells
fibroblast-like stromal cells

PLACENTAL OXIDATIVE STRESS has been implicated in the pathogenesis of pregnancy-related complications such as miscarriage, preterm delivery, and preeclampsia (Hubel 1999; Burton and Jauniaux 2004). Highly reactive products of lipid peroxidation are formed when free radicals attack polyunsaturated fatty acids or cholesterol in lipoproteins. Oxidized low-density lipoprotein (ox-LDL) is a major product of lipid peroxidation. Elevated levels of antibodies to ox-LDL in women with established preeclampsia and in pregnant women with a history of repeated abortion indicate that uncontrolled lipid peroxidation and impaired ox-LDL elimination may induce cellular dysfunction and damage in the placenta (Branch et al. 1994; Tulppala and Ailus 1995). In isolated normal trophoblasts and placental macrophages, cellular uptake and degradation of modified LDL (scavenger receptor activity) were 20-fold higher than those of LDL (Bonet et al. 1995). Such scavenger receptor activity in the placenta may function to degrade modified lipoproteins and prevent toxic effects on placental cellular function and fetal growth and development (Bonet et al. 1995).

Lectin-like ox-LDL receptor-1 (LOX-1) is one of the scavenger receptors that is mainly expressed in vascular endothelial cells (Sawamura et al. 1997). It was initially cloned from bovine aortic endothelial cells and from human lung as a novel receptor for ox-LDL (Sawamura et al. 1997). LOX-1 shows strong activity for binding, internalizing, and degrading ox-LDL (Moriwaki et al. 1998b). It is induced by stimuli including angiotensin II (Li et al. 1999), tumor necrosis factor-α (Kume et al. 1998), and advanced glycation end products (Chen et al. 2001), as well as ox-LDL itself (Aoyama et al. 1999). LOX-1 is involved in ox-LDL–induced apoptosis of vascular endothelial cells through intracellular production of reactive oxygen species (Li and Mehta 2000).

Correspondence to: Motohiro Takeya, Department of Cell Pathology, Graduate School of Medical Sciences, Kumamoto University, 1-1-1 Honjo, Kumamoto 860-8556, Japan. E-mail: takeya@kumamoto-u.ac.jp

Received for publication December 15, 2007; accepted April 23, 2008 [DOI: 10.1369/jhc.2008.950543].

0022-1554/08/$3.30